Plant Communications
Research article

CellPress
Partner Journal

Bacterial community-emitted volatiles regulate *Arabidopsis* growth and root architecture in a distinct manner of those from individual strains

Gözde Merve Türksoy[1,2], Miroslav Berka[3], Kathrin Wippel[1,4], Anna Koprivova[2], Réjane Audrey Carron[1], Lioba Rüger[1], Martin Černý[3], Tonni Grube Andersen[1,*] and Stanislav Kopriva[2,*]

[1]Max Planck Institute for Plant Breeding Research, Carl-von-Linne-Weg 10, 50829 Cologne, Germany

[2]Institute for Plant Sciences, Cluster of Excellence on Plant Sciences (CEPLAS), University of Cologne, Cologne 50674, Germany

[3]Department of Molecular Biology and Radiobiology, Faculty of AgriSciences, Mendel University in Brno, Brno, Czech Republic

[4]Swammerdam Institute for Life Sciences, Faculty of Science, University of Amsterdam, Science Park 904, 1098 XH Amsterdam, the Netherlands

***Correspondence: Tonni Grube Andersen (tandersen@mpipz.mpg.de), Stanislav Kopriva (skopriva@uni-koeln.de)**

https://doi.org/10.1016/j.xplc.2025.101351

ABSTRACT

Volatile organic compounds (VOCs) function as infochemicals and are important means of communication between bacteria and plants. Bacterial VOCs can promote plant growth and protect plants against both biotic and abiotic stresses. Most studies to date have focused on VOCs from single bacterial strains; consequently, very little is known about VOCs emitted by bacterial communities and their role in modulating plant phenotypes. In this work, we showed that VOCs from a root-derived 16-strain synthetic community affect *Arabidopsis* growth and root system architecture, whereas VOCs from individual strains produce a range of different effects. Removal of key species from the community changed the relative abundances of other strains and altered the VOC composition; however, the effect on plant growth remained the same. We therefore concluded that bacterial VOC-induced modulation of plant responses in the rhizosphere may be an emergent property of bacterial communities, rather than merely the sum of effects exerted by individual species. In total, we detected 135 different volatiles from individual strains, with dimethyl disulfide (DMDS) being the most abundant compound emitted by the community. Correlation analysis predicted several sulfur-containing compounds to promote plant growth, and revealed that exposure to two such VOCs, along with DMDS, leads to plant growth promotion. We also identified plant mutants unresponsive to DMDS, suggesting that its mechanism of action may involve assimilation into S-methylcysteine. Finally, we propose that the ecological role of VOCs is to provide early signaling alerts that prime plants for interaction with the bacterial community through modulation of root exudate composition and accumulation of defense compounds, thereby affecting the bacterial colonization of the plants.

Key words: *Arabidopsis*, bacterial volatiles, synthetic communities, sulfur, dimethyl disulfide, plant–microbe interactions

Türksoy G.M., Berka M., Wippel K., Koprivova A., Carron R.A., Rüger L., Černý M., Andersen T.G., and Kopriva S. (2025). Bacterial community-emitted volatiles regulate *Arabidopsis* growth and root architecture in a distinct manner of those from individual strains. Plant Comm. **6**, 101351.

INTRODUCTION

In nature, the roots of healthy plants associate with a diverse set of microorganisms, collectively termed the root microbiota (Bulgarelli et al., 2013; Bai et al., 2015). These communities of microbes—particularly bacteria—benefit their host by protecting against abiotic and biotic stresses and promoting growth through nutrient acquisition and modulation of host phytohormone levels (Trapet et al., 2016; Castrillo et al., 2017; Zhang et al., 2019; Harbort et al., 2020; Piechulla et al., 2017). In addition, plants use short-range communication to shape their microbiome by secreting belowground metabolites known as root exudates (Stringlis et al., 2018; Koprivova and Kopriva, 2022; Basak et al., 2024). Although most attention has focused on communication from the plant to the microbiome, this interaction is bidirectional. One important mode of

communication involves volatile organic compounds (VOCs) emitted by bacteria. Due to their low molecular mass, low boiling point, and high vapor pressure, VOCs can act as both long- and short-range signals via air, water, and soil (Schulz and Dickschat, 2007). Bacterial VOCs are chemically diverse and can make up complex "bouquets" of compounds with emergent properties and overlapping effects that depend on the growth substrate and environmental conditions (Blom et al., 2011; Fincheira and Quiroz, 2018). These VOCs are derived from major biosynthetic pathways, including primary metabolism, fermentation, sulfur metabolism, fatty acid metabolism, and terpene synthesis (Schulz and Dickschat, 2007; Peñuelas et al., 2014; Weisskopf et al., 2021). For example, VOCs produced through primary metabolism include derivatives of valine, leucine, and isoleucine, such as 2-methylbutanoic acid, 3-methylbutanoic acid, and methylpropanoic acid (Peñuelas et al., 2014). These compounds tend to be common components of VOC bouquets rather than being specific to a limited number of bacterial strains (Ryu et al., 2020). In contrast, 1-undecene, produced by the fatty acid pathway (Popova et al., 2014; Lo Cantore et al., 2015), is limited to *Pseudomonas* strains. VOCs produced through secondary metabolism include bacterial family-specific compounds, such as 2,5-diisopropylpyrazine, which is produced from valine by *Paenibacillus polymyxa* and *Chondromyces* (Beck et al., 2003; Schulz and Dickschat, 2007; Blom et al., 2011), and the terpenoid geosmin, produced by actinobacteria, myxobacteria, and cyanobacteria (Martín-Sánchez et al., 2019). Some VOCs are even strain-specific, such as sodorifen, produced through the terpene biosynthesis pathway by *Serratia plymuthica* (Weise et al., 2014), and the polyketide streptopyridine from *Streptomyces* (Groenhagen et al., 2014). Others are widely produced across the bacterial kingdom, such as the sulfur-containing VOCs dimethyl sulfide, dimethyl disulfide (DMDS), and dimethyl trisulfide, and the aromatic compounds indole and 2-phenylethanol (Ryu et al., 2020; Weisskopf et al., 2021).

A large number of bacterial strains have been reported to modulate plant growth, leading to increased biomass and changes in root system architecture (Ryu et al., 2003; Groenhagen et al., 2013). One of the best-characterized bacterial models for such plant growth promotion (PGP) studies is *Pseudomonas simiae* WCS417 (Pieterse et al., 2021), a strain first isolated from the wheat rhizosphere that triggers direct plant growth promotion and induces systemic resistance in the host (Pieterse et al., 1996; Knoester et al., 1999). WCS417 acts as a biocontrol agent by suppressing wheat disease caused by the soil-borne fungus *Gaeumannomyces graminis* var. *tritici* (Lamers et al., 1988). It also protects plants from abiotic stress; e.g., it increases drought resistance in peppermint (Chiappero et al., 2019) and salt tolerance in *A. thaliana* (Loo et al., 2022). Moreover, VOCs produced by WCS417 promote plant growth and induce changes in root architecture, increasing lateral root and root hair density in a manner comparable to direct bacterial contact (Blom et al., 2011; Zamioudis et al., 2013). Most VOC-related studies have been conducted with single bacterial strains, or they have used low-diversity bacterial communities and focused on community richness effects (Raza et al., 2021) or on their ability to suppress disease in natural environments (Gfeller et al., 2022). Bacterial VOCs are also important to natural ecosystems, e.g., for modulating insect behavior and plant attractiveness to insects (Zhang et al., 2024). Interestingly, the strongest PGP effects have been observed at the lowest community richness, whereas intermediate richness promoted pathogen suppression by VOCs (Raza et al., 2020). Similarly, reduced community diversity increased overall VOC emissions from soil but decreased the number of distinct VOCs produced (Abis et al., 2020). However, another study reported that increasing species richness within a bacterial family increased both pathogen suppression and PGP (Wang et al., 2021). Therefore, the framework for understanding VOC-mediated modulation of plants by root-associated bacterial communities under conditions resembling natural environments seems to still be underdeveloped (Weisskopf et al., 2021). Synthetic communities (SynComs) that represent the phylogenetic diversity of natural soil bacteria provide a powerful tool to investigate plant–microbe interactions and microbiome functions, including the role of bacterial VOCs (Vorholt et al., 2017; Martins et al., 2023). For example, SynComs composed of 16 bacterial families isolated from *Arabidopsis* roots have been used to demonstrate host preference for commensal bacteria (Wippel et al., 2021).

In this work, we investigate how VOCs derived from root microbiome bacterial communities affect *Arabidopsis* growth and root architecture. Using a 16-member SynCom, we show that bacteria–bacteria interactions affect community VOC profiles, leading to emergent properties in the resulting VOC bouquets. We identify several VOCs with PGP properties and propose a mechanism by which DMDS promotes plant growth. We suggest that bacterial VOCs may function as signaling compounds that prime plants for interactions with the bacterial community through modulation of root exudate composition and accumulation of defense compounds.

RESULTS

VOCs from a 16-member SynCom and its individual strains affect *Arabidopsis* growth and root architecture

To study how bacterial VOCs affect *Arabidopsis* seedlings, we chose a previously established and characterized 16-member SynCom (16 SC) (Wippel et al., 2021). This SynCom consists of strains from 16 bacterial families selected from the At-RSPHERE strain library, isolated from the roots of *Arabidopsis* plants grown in natural soil (Bai et al., 2015). These families cover a broad taxonomic range and are also found in the roots of other plant species (Bai et al., 2015; Wippel et al., 2021) (Supplemental Figure 1B). By cultivating plants alone (control), with bacteria mixed into the plant growth medium (direct bacterial contact [DBC]), with bacteria in a separate compartment (non-bacterial contact [NBC]), and with both DBC and NBC (Supplemental Figure 1A), we assessed the extent to which 16 SC modulates plant growth. In line with previous findings (Durán et al., 2018; Wippel et al., 2021), in the DBC configuration, 16 SC significantly increased the whole-plant fresh weight compared with the control (Figure 1A; Supplemental Figure 2). Intriguingly, in the NBC and combined configurations, the fresh weight was also significantly increased (Figure 1A); however, unlike the DBC configuration, both treatments led to a significant decrease in primary root length

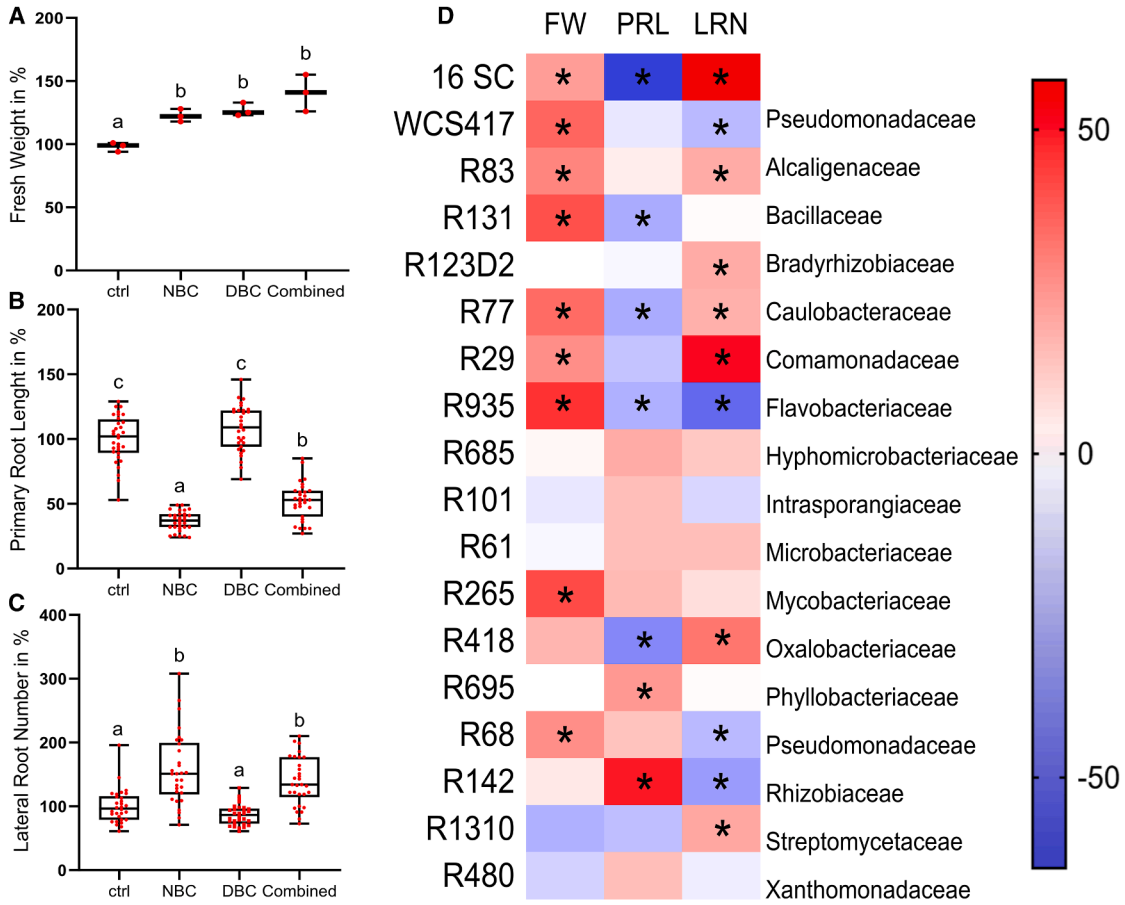

Figure 1. Effects of bacterial VOCs on *Arabidopsis* growth and root system architecture.

(A–C) Five-day-old *Arabidopsis thaliana* seedlings were transferred to MS-agar Petri dishes and grown for 10 days under 4 conditions: without bacteria as a control (ctrl), in a shared headspace with 16 SC (NBC), with 16 SC in the agar in direct bacterial contact (DBC), or in a combination of both exposure types (Combined) (cf. Supplemental Figure 1).

(A) Fresh weight of whole seedlings compared with the control (ctrl = 100%); mean of 3 pooled samples with at least 10 seedlings each.

(B) Primary root length compared with the control (ctrl = 100%); mean of 30 plants.

(C) Lateral root number compared with the control (ctrl = 100%); mean of 30 plants. **(A–C)** Data are shown as boxplots: the central bar indicates the median, the lower and upper box limits indicate the 25th and 75th percentiles, respectively; whiskers indicate the minimum and maximum values; dots indicate individual samples. Different letters indicate statistically significant differences: one-way ANOVA with Tukey's HSD test **(A)**, Welch and Brown–Forsythe tests with Dunnett's test **(B)**, and Kruskal–Wallis with Dunnett's test **(C)**; $p < 0.05$.

(D) Heatmap showing the effects of 16 SC, its individual component strains, and *Pseudomonas simiae* WCS417 on *Arabidopsis* fresh weight (FW), primary root length (PRL), and lateral root number (LRN) after 10 days of growth with VOC exposure in the NBC setup. Results are shown as percentages relative to the control without bacteria, based on means of 3 biological replicates containing 10 seedlings each. Asterisks indicate statistically significant differences compared with the control (Student's *t*-test, $p < 0.05$). For absolute data, see Supplemental Figure 3.

(PRL) and a concurrent increase in lateral root number (LRN) (Figure 1B and 1C). These results indicate that VOCs produced by a root-associated bacterial community promote plant growth and modulate root architecture.

To disentangle these effects, we examined how individual members of 16 SC affected *Arabidopsis* plants in the NBC configuration. As a positive control, we used the *Pseudomonas* strain WCS417, known to promote growth in *Arabidopsis* seedlings through VOCs (Zamioudis et al., 2015; Pieterse et al., 2021). Interestingly, among the 16 strains included in 16 SC, only R77 affected fresh weight, PRL, and LRN in the same manner as 16 SC, whereas VOCs from 4 strains (R685, R101, R61, and R480) had no significant effects (Figure 1D; Supplemental Figure 3). VOCs from 7 strains (R83, R131, R77, R29, R935, R265, and R68) and WCS417 significantly increased total fresh weight, similar to 16 SC (Figure 1D). VOCs from 4 strains (R131, R77, R935, and R418) reduced PRL, similar to 16 SC, whereas R695 and R142 had the opposite effect and increased PRL (Figure 1D). Six strains (R83, R123D2, R77, R29, R418, and R1310) promoted LRN, similar to 16 SC, whereas WCS417, R935, R68, and R142 reduced LRN compared with controls (Figure 1D). These results allowed us to classify the strains into those that produced plant growth-promoting VOC blends (PGPs) and those that did not (non-PGPs). Taken together, the individual strains elicited a range of responses affecting shoot biomass and/or root architecture that were distinct from those of 16 SC. These findings suggest that the plant response to 16 SC may result from specific key strains,

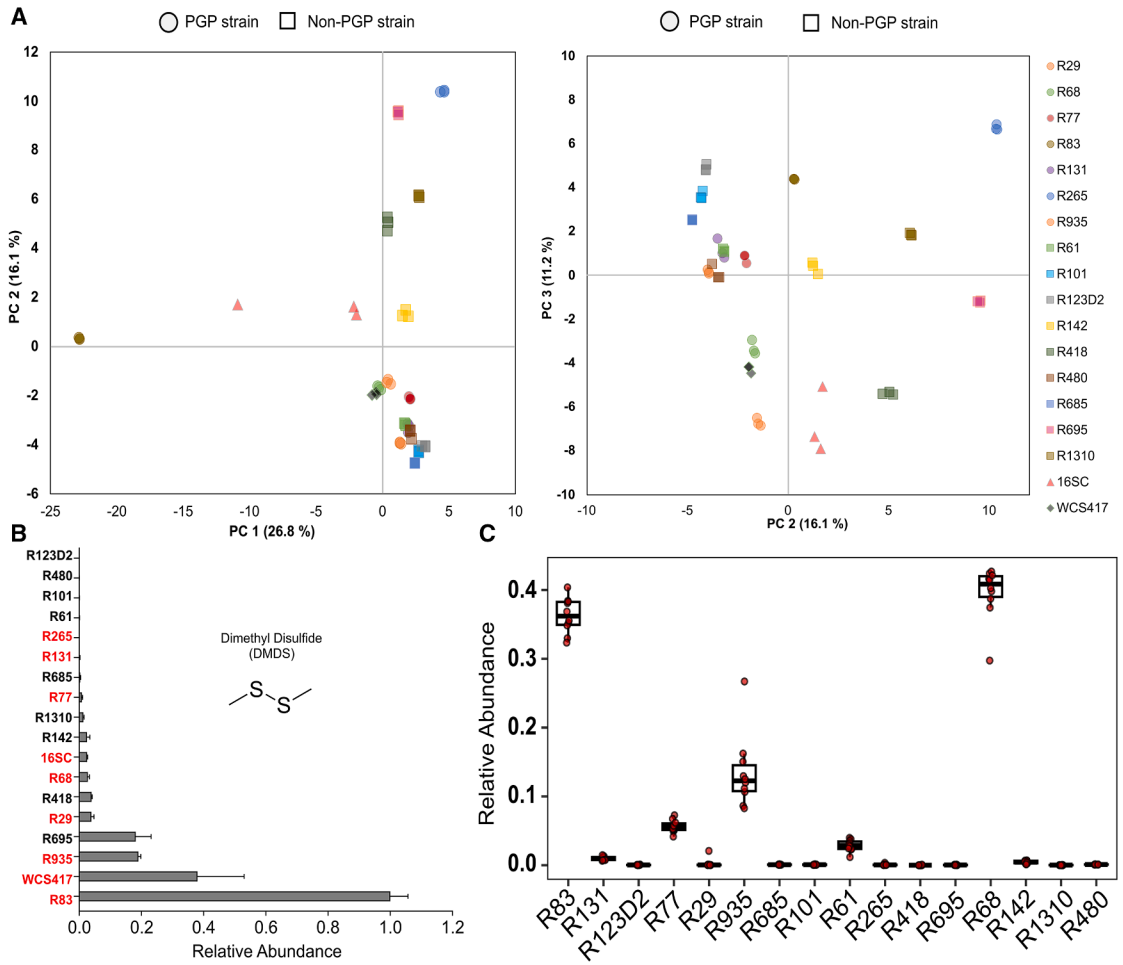

Figure 2. VOC profiles of individual strains.

(A) 16 SC, its individual component strains, and the control strain *Pseudomonas* WCS417 were grown on TSB medium for 2 days. VOCs were captured using SPME and analyzed by GC–MS. PCA of all 135 identified volatiles from 3 biological replicates was performed using ClustVis. Colored circles and squares indicate plant growth-promoting (PGP) and non-PGP strains, respectively.

(B) Relative abundance of dimethyl disulfide (DMDS) produced by individual strains and 16 SC, determined via SPME capture and GC–MS. Values are based on peak areas from 3 biological replicates. The means and standard deviations of the peak areas are normalized to 16 SC, which was set to 1. Red indicates strains that produce a plant growth-promoting VOC blend.

(C) Relative abundance of individual 16 SC strains based on 16S rRNA gene profiling from 6 biological replicates. Data are shown as boxplots: the central bar indicates the median; the lower and upper box limits indicate the 25th and 75th percentiles, respectively; dots indicate individual samples.

or it may be an emergent property arising from species interactions within the mixed community.

GC–MS analysis reveals distinct yet overlapping VOC profiles in communities and individual strains

Next, to identify compounds that might affect plant phenotypes, we conducted gas chromatography–mass spectrometry (GC–MS) analysis of the VOCs emitted by 16 SC and its individual strains. In total, 135 different VOCs were detected, including sulfur-containing volatiles, terpenes, alcohols, and ketones (Supplemental Table 1). The VOC blend from 16 SC contained 55 compounds, whereas the number emitted by individual strains ranged from 5 VOCs in R101 to 62 in R83. Therefore, not all compounds emitted by individual strains were present in the 16 SC VOC bouquet. Principal component analysis (PCA) of the VOC profiles showed that each strain had a distinct profile, and all of them differed from that of 16 SC (Figure 2A). R83 not only produced the highest number of VOCs but also exhibited the most distinct VOC profile (Figure 2A), likely due to several unidentified terpene compounds unique to this strain (Supplemental Table 1). Fifty-seven compounds were unique to a single strain, whereas two sulfur-containing VOCs, DMDS and dimethyl trisulfide, were detected in all strains, though at varying levels (Supplemental Table 1). As DMDS is known to promote plant growth (Meldau et al., 2013; Tyagi et al., 2019), it is not surprising that the highest DMDS emitters were the PGP strains R83, R935, and WCS417, all of which emitted more DMDS in monoculture than 16 SC (Figure 2B) (Meldau et al., 2013; Tyagi et al., 2019). In contrast, strains emitting DMDS at levels similar to 16 SC included both PGP strains (R29, R68, and R77) and non-PGP strains (R418, R142, and R1310). Strains emitting low levels of DMDS were mostly non-PGP strains (R685, R61,

R101, R480, and R123D2), with the exceptions of R265 and R131 (Figure 2B). Therefore, DMDS is unlikely to be solely responsible for the *Arabidopsis* growth modulation induced by 16 SC VOCs.

To determine which strains drove the VOC profile of 16 SC, we analyzed the community composition after 10 days of growth using 16S rRNA gene amplicon sequencing. Interestingly, although the community was assembled using equal proportions of all 16 strains, after 10 days, it was dominated by R83, R935, and R68 (Figure 2C). These three strains collectively accounted for about 90% of the bacterial DNA detected in the community. Therefore, although the individual strains exhibit complex VOC profiles with both shared and unique compounds, the community VOC profile may be formed by a few dominant strains.

VOCs emitted by communities have beneficial effects beyond the combination of individual strains

To determine whether the dominant bacterial strains R935, R83, and R68 were responsible for the effects of 16 SC VOCs on plants, we performed drop-out experiments in which these strains were individually or jointly omitted from the SynCom. These reduced communities were then grown with plants in the NBC configuration. In all drop-out combinations, the fresh weight of exposed plants was significantly higher than that of the control (Figure 3A). We also observed a significant reduction of PRL in all combinations (Figure 3B). Therefore, the effect of VOCs from the full SynCom on plants is likely an emergent property of the bacterial community and not the result of a few dominant strains. We then tested whether the less-abundant strains might have important contributions to the community VOC profile by exposing plants to VOCs from 16 SC drop-outs missing PGP strains R265 and R131 or the non-PGP strain R123D2 (Figure 1D). As with the previous drop-out communities, these retained the same PGP properties as 16 SC when compared with the R935 drop-out as a control (Supplemental Figure 4). Therefore, the loss of one or more strains does not significantly alter the effect of 16 SC VOCs on *Arabidopsis* growth.

Because the drop-out communities had the same effect on plants as the full 16 SC, we examined whether and how their VOC profiles changed. Overall, there were clear differences in VOC composition (Figure 3C; Supplemental Table 2). DMDS was the dominant VOC in most of the drop-out communities (Figure 3D), except in those omitting R935 or both R935 and R83. However, further exclusion of R68 restored DMDS abundance (Figure 3D). Interestingly, loss of the highest DMDS producer, R83, did not reduce DMDS concentration compared with the full 16 SC. In contrast, terpene and undecene production was lost in the absence of R83 and R68, respectively (Figure 3D).

Because removal of the dominant strains only moderately affected the profiles of major VOCs, we investigated how their absence affected community composition using 16S rRNA profiling. PCA of beta-diversity (Bray–Curtis dissimilarities) showed a clear separation of the drop-out communities (Supplemental Figure 5A). Removal of the three dominant strains had a strong impact on community structure but did not appear to affect the observed VOC-mediated effects on plants. The dominant strains R935, R68, and R83 continued to dominate the drop-out communities unless all three were removed (Supplemental Figure 5B). For quantitative analysis, we adjusted the relative abundance (RA) in each 16 SC drop-out community by *in silico* removal of reads corresponding to the omitted strains before the RA calculation. Interestingly, removal of R68 led to increased RA of R83, and conversely, removal of R83 led to increased RA of R68, whereas removal of R935 had no effect on either strain (Figure 3E). However, removal of the dominant strains also affected the RAs of other strains compared with the full 16 SC (Figure 3E). For example, removal of R68 and R83, with or without R935, increased the RA of R101, a non-PGP strain. Likewise, removal of R935 increased the RA of the PGP strain R77. The greatest effect on the RAs of other strains was observed when all three dominant strains were removed, although omission of R83 and R68 alone produced similar effects (Figure 3E). Nevertheless, despite these large changes in bacterial abundances and community composition, the emitted VOC blends continued to influence the plant in a similar manner to the full SynCom. This suggests that the community may adjust its composition and/or metabolism to produce a growth-promoting VOC blend that acts as more than just the sum of its parts.

To further investigate these emergent properties, we analyzed two partial SynComs composed exclusively of either the PGP or non-PGP strains (Figure 1D). VOCs from both groups triggered significant growth promotion, similar to that of 16 SC (Figure 4A). Similarly, VOCs from both groups led to significantly shorter PRL, though not to the same degree as VOCs from 16 SC (Figure 4B). Comparison of the community compositions revealed that removal of the nine non-PGP strains did not alter the dominance of R83, R935, and R68 in the PGP community (Figure 4C). The non-PGP community, composed of those nine strains, was dominated by R101, R142, and R61. The RAs of R101 and R142 increased in most of the drop-out communities, which indicates that they might be suppressed by the dominant strains in the full 16 SC. VOC profiling showed that both communities emitted DMDS at levels similar to 16 SC. However, only the PGP community produced 1-undecene and terpenes, because the respective producers of these VOCs, R68 and R83, were present only in that group (Figure 4D; Supplemental Table 2). In summary, a combination of strains that individually do not promote growth can still result in growth promotion and similar root system changes, supporting the conclusion that bacterial communities as a whole exhibit emergent properties beyond the additive effects of individual strains.

Characterization of plant growth promoting volatiles from 16-member SynCom

To identify additional putative PGP volatiles, we correlated the VOC data with the changes in plant fresh weight (Figure 5A; Supplemental Table 3). Variable importance in projection (VIP) values suggested that three compounds, 2-methyl-5-(methylthio)-furan (2M5MTF), 2-methyl-5-(methylthio)-thiophene, and 2,4-dithiapentane (2,4-DTP), may possess PGP activity in *Arabidopsis*. We selected 2M5MTF and 2,4-DTP for further testing, along with three other VOCs: the ubiquitous DMDS, S-methyl thiobutyrate (SMTB), and the well-characterized antifungal and anti-oomycete VOC 1-undecene (C11:1) (Hunziker et al., 2015;

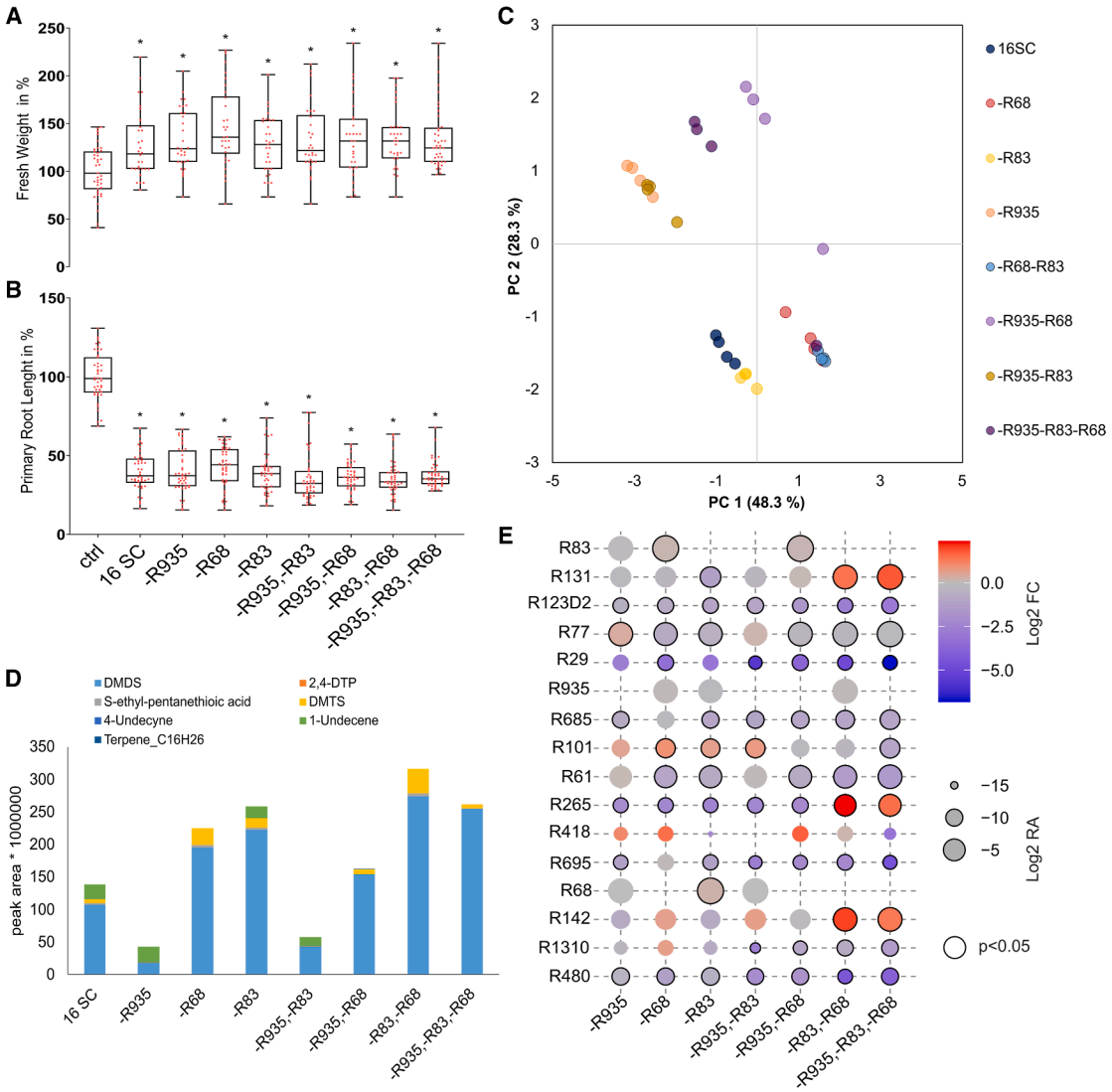

Figure 3. Characterization of drop-out communities.

(A–B) *Arabidopsis* plants were grown for 10 days in the NBC setup in a shared headspace with the full 16 SC, drop-out communities where the highly abundant strains were individually or jointly omitted, or without bacteria (ctrl). Shoot fresh weight **(A)** and primary root length **(B)** were measured in 4 replicate plates, each containing 10 plants. Results are expressed as percentages relative to the control and shown as boxplots, with individual values indicated by red dots. Asterisks indicate statistically significant differences compared with the control (Kruskal–Wallis with Dunnett's test, $p < 0.05$, $n = 40$).

(C) PCA of 7 VOCs identified with high confidence by headspace GC–MS analysis of VOCs produced by the drop-out communities after 1 day of growth on TSB medium, based on 4 biological replicates.

(D) Relative abundance of the 7 VOCs identified by headspace GC–MS analysis of VOCs produced by the 16 SC and drop-out communities after 1 day of growth on TSB medium, based on peak areas from 4 biological replicates.

(E) Dot plot showing the relative abundance (RA) of each strain in the drop-out communities compared with the full 16 SC, based on rRNA profiling of 9 biological replicates. Dot size corresponds to the $\log_2$ mean RA; color indicates the $\log_2$ fold change in RA relative to 16 SC after *in silico* depletion of the relevant strain(s) (see Materials and methods). Circled dots indicate statistically significant changes (Wilcoxon rank sum test, $p < 0.05$).

Lo Cantore et al., 2015). To determine whether these VOCs were responsible for the observed plant phenotypes, we used pure compounds instead of SynComs in the NBC setup. As previously reported (Tyagi et al., 2019), the application of 50 µl of 50 µM DMDS significantly promoted growth, similar to 16 SC (Figure 5B). The same was true for 2M5MTF and 2,4-DTP, as predicted (Figure 5A). In contrast, neither SMTB nor 1-undecene affected *Arabidopsis* fresh weight (Figure 5B). Interestingly, when tested at different concentrations, all of the growth-promoting VOCs except 2,4-DTP lost this effect at the highest concentration (500 µM), and SMTB was toxic at high concentration (Supplemental Figure 6). Overall, these results show that multiple individual VOCs may contribute to the effect of 16 SC VOCs on shoot growth.

Because DMDS is a ubiquitous VOC and its sulfur can be assimilated by plants (Meldau et al., 2013), we investigated the mechanisms underlying its PGP effect. DMDS is converted to

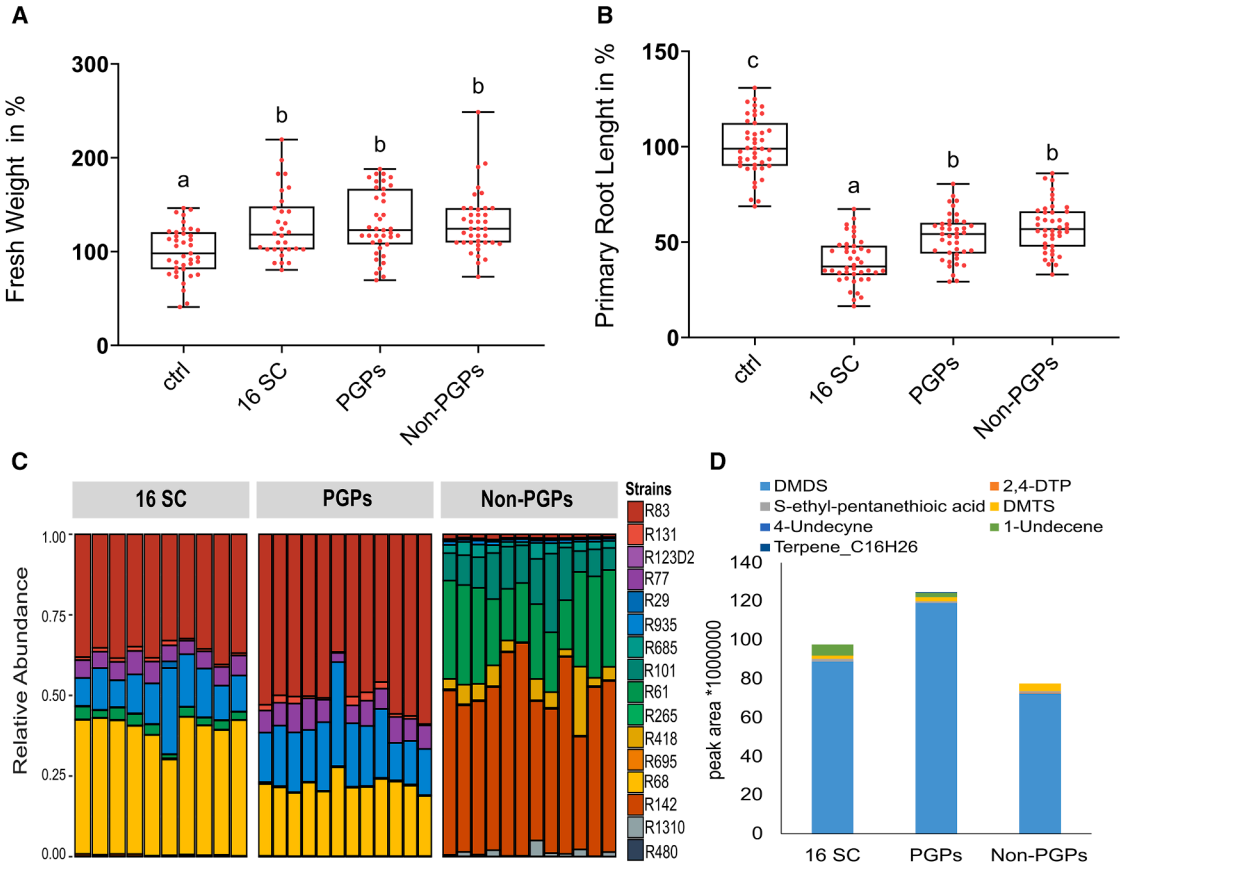

Figure 4. Analysis of PGP and non-PGP communities.

Arabidopsis plants were grown for 10 days in the NBC setup in a shared headspace with 16 SC, or with communities formed from all PGP strains (PGPs) or all non-PGP strains (non-PGPs) from 16 SC. Shoot fresh weight **(A)** and primary root length **(B)** were measured in 4 replicate plates, each containing 10 plants. Results are expressed as percentages relative to the control and shown as boxplots with individual values indicated by red dots. Different letters indicate statistically significant differences (one-way ANOVA with Tukey's HSD test, $p < 0.05$, $n = 40$).

(C) Relative abundance of bacterial strains in each community, determined by 16S rRNA gene profiling.

(D) Relative abundance of the 7 VOCs in the 16 SC, PGP, and non-PGP communities, determined by headspace GC–MS analysis after 1 day of growth on TSB medium, based on peak areas from 4 biological replicates.

methanethiol, a naturally occurring plant metabolite derived from methionine degradation by methionine γ-lyase (MGL) (Figure 5C) (Rébeillé et al., 2006). Methanethiol can be further degraded to hydrogen sulfide, formaldehyde, and hydrogen peroxide by methanethiol oxidase (MTO), which in animals is carried out by selenium-binding proteins (SELENBPs) (Philipp et al., 2023). Alternatively, it can be incorporated into O-acetylserine (OAS), the precursor of cysteine, to form S-methylcysteine (Rébeillé et al., 2006). To determine which of these reactions contribute to DMDS-induced growth promotion, we assessed the effect of DMDS in *Arabidopsis* mutants defective in these pathways. The *sbp1* (defective in the SELENBP homolog) and *mgl* mutants showed DMDS-induced increases in growth similar to the wild-type (WT) Col-0 (Figure 5D), which makes MTO an unlikely route for DMDS assimilation. In contrast, two mutants in O-acetylserine(thiol)lyase—*oastlA* and *oastlBC*, which disrupt the main cytosolic isoform and both plastidic and mitochondrial isoforms, respectively (Wirtz and Hell, 2006; Watanabe et al., 2008)—did not benefit from DMDS exposure (Figure 5D). These results suggest that the OAS pathway is essential for this effect. This conclusion was further supported by the loss of growth promotion in *serat2;2*, a mutant that lacks the mitochondrial isoform of serine acetyltransferase, the enzyme that synthesizes OAS, the putative acceptor of methanethiol (Figure 5D). These findings suggest that DMDS from 16 SC (and other bacteria) is incorporated into the plant's organic sulfur pool through a reaction with OAS, resulting in S-methylcysteine. However, the subsequent fate of this compound is unknown. The *oastlA* and *oastlBC* mutants still exhibited increased growth upon exposure to VOCs from 16 SC (Supplemental Figure 7), providing further evidence that the PGP effect of 16 SC VOCs is multifactorial and mediated by multiple compounds.

VOCs act as early signals to prime bacterial colonization of plants

We then considered the physiological relevance of bacterial VOC signaling. We hypothesized that bacterial VOCs may prime plants for subsequent microbial interactions, and thus VOC-treated plants would assemble a different community. To test this, we first grew plants for 5 days with or without exposure to 16 SC

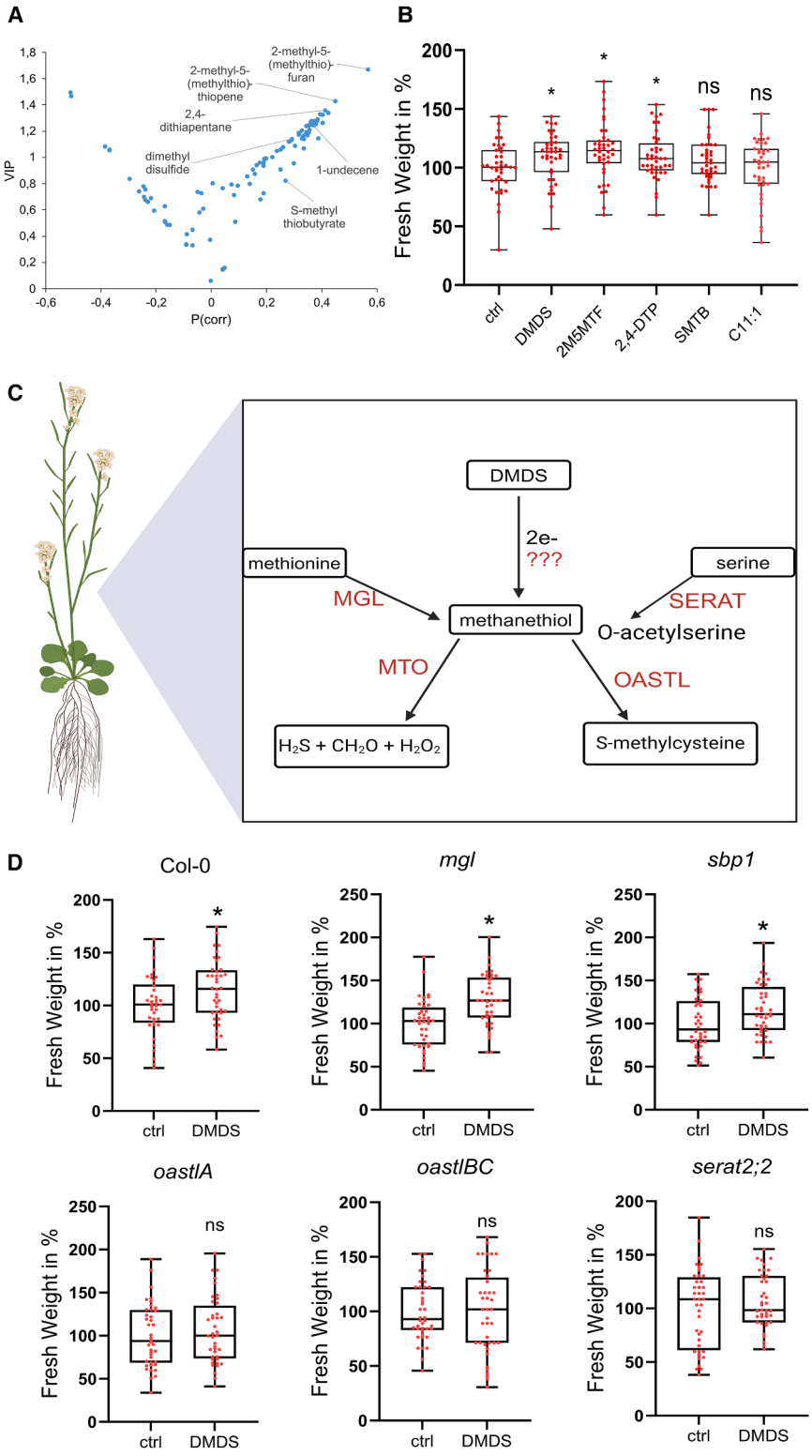

Figure 5. Effects of pure VOCs on plants.

(A) Candidate VOCs associated with growth responses in *Arabidopsis*. The variable importance in projection (VIP) plot was derived from orthogonal partial least-squares analysis, using growth response as the predictor. VIP scores are plotted against Pearson correlation coefficients (*p*(corr)) from correlations between plant fresh weight and the peak area of each VOC. VOCs with abundance significantly correlated with growth are labeled.

(B) *Arabidopsis* plants were grown for 10 days in a shared headspace with 16 SC or with 50 µl of the following VOCs: 50 µM DMDS, 10 µM 2-methyl-5-(methylthio)furan (2M5MTF), 50 µM 2,4-dithiapentane (2,4-DTP), 10 µM S-methyl thiobutyrate (SMTB), or 50 µM 1-undecene (C11:1). Shoot fresh weight was determined in 40 plants. Results are expressed as percentages relative to the control and shown as boxplots with individual values indicated by dots. Asterisks indicate statistically significant differences compared with the control (Student's *t*-test, $p < 0.05$, $n = 40$). ns, not significant.

(C) Proposed scheme of reactions involved in DMDS assimilation.

(D) Wild-type Col-0 and the mutants *mgl*, *sbp1*, *oastlA*, *oastlBC*, and *serat2;2* were grown for 10 days in a shared headspace with 50 µl of 50 µM DMDS. Shoot fresh weight was determined in 40 plants. Results are expressed as percentages relative to the control and shown as boxplots with individual values indicated by dots. Asterisks indicate statistically significant differences compared with the control (Student's *t*-test, $p < 0.05$, $n = 40$). ns, not significant.

VOCs, then transferred them to DBC or control conditions for another 7 days. The VOC pre-treatment resulted in PGP regardless of the presence of 16 SC in the agar (Figure 6A). We then analyzed the composition of root-associated microbes using 16S rRNA profiling. Pre-treatment with 16 SC VOCs significantly altered the composition of the root-associated community. Surprisingly, in the control plants, after 7 days on 16 SC plates, the root microbiome was dominated by R68, which accounted for approximately 90% of all reads. In contrast, in plants pre-exposed to 16 SC VOCs, the root-associated community was significantly different, with increased RAs of R101, R131, and R1310 (Figure 6B). These findings suggest that VOCs prime plants for bacterial colonization. Interestingly, pre-exposure to DMDS under the same conditions did not promote growth or affect the root-associated community (Supplemental Figure 8).

We then hypothesized that VOCs trigger metabolic changes in plants, for example by altering the synthesis of plant defense compounds or the composition of root exudates, thereby facilitating bacterial colonization. To test this, we measured the levels of defense compounds, namely glucosinolates and camalexin, in the shoots of plants exposed to 16 SC or the model bacterial strain *Pseudomonas* WCS417 in the

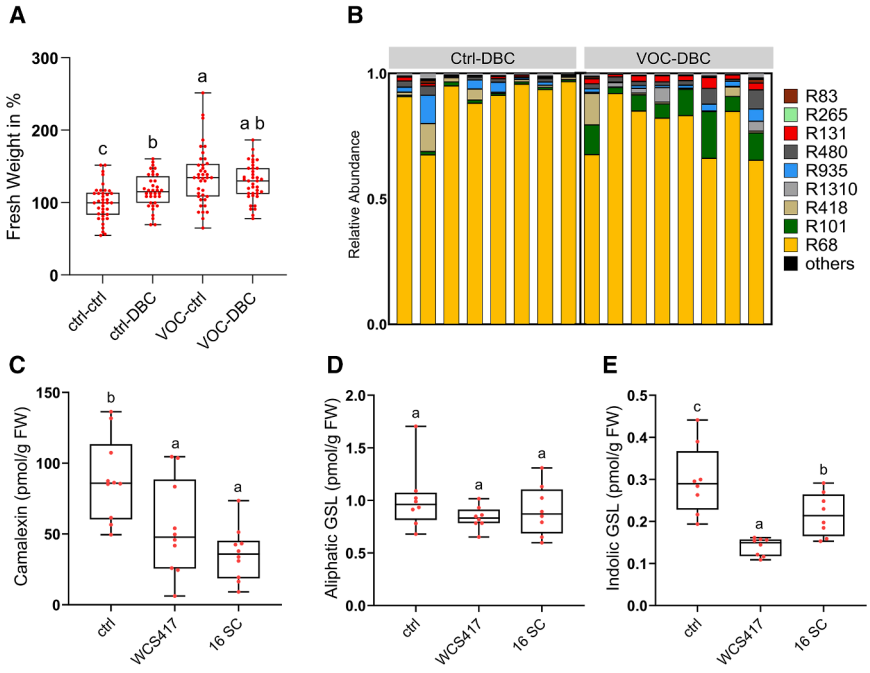

Figure 6. Priming by VOCs.

Arabidopsis plants were grown for 5 days on MS–agar plates, with or without sharing headspace with 16 SC. Plants were then transferred to plates with or without direct contact with 16 SC and grown for an additional 7 days.

(A) FW of primed (VOC–DBC, VOC–ctrl), non-primed (ctrl–DBC), and control plants (ctrl–ctrl) was determined. Results are expressed as percentages relative to the control and shown as boxplots with individual values indicated by dots. Different letters indicate statistically significant differences (Welch and Brown–Forsythe tests with Dunnett's test, $p < 0.05$, $n = 10$).

(B) Root community composition was analyzed by 16S rRNA gene profiling. The chart shows the RA of bacterial strains in the root communities of plants primed or not primed with 16 SC VOCs.

(C–E) *Arabidopsis* plants were grown for 10 days in a shared headspace with 16 SC, *Pseudomonas* WCS417, or no bacteria (control). The amounts of camalexin **(C)**, aliphatic glucosinolates **(D)**, and indolic glucosinolates **(E)** were quantified by HPLC in eight independent pools of three shoots. Results are shown as boxplots with individual values indicated by dots. Different letters indicate statistically significant differences (one-way ANOVA with Tukey's HSD test, $p < 0.05$, $n = 8$). ns, not significant.

NBC setup, along with untreated controls. Although the levels of aliphatic glucosinolates after VOC exposure were unchanged, the levels of indolic glucosinolates and camalexin were reduced (Figure 6C–6E). To gain deeper insight into VOC-induced metabolic alterations, we performed a GC–MS analysis of *Arabidopsis* exudates, roots, and shoots at 2 and 5 days after exposure to 16 SC VOCs. We quantified a total of 102 metabolites, of which 71 were detected in the exudates, including many sugars, amino acids, organic acids, and several defense-related compounds (Figure 7). Exposure to 16 SC VOCs affected metabolite composition not only in the exudates, but also in both roots and shoots, with a clear temporal dynamic. In the exudates, changes were more pronounced after 5 days, with the majority of metabolites being less abundant in VOC-treated plants than in the controls. However, remarkably, except for tricarboxylic acid cycle intermediates (such as citrate, oxoglutarate, and malate) and the amino acids aspartate and glutamate, most metabolites were more abundant in the exudates after 2 days and less abundant after 5 days of VOC exposure, when compared with the respective controls (Figure 7; Supplemental Table 4). After 5 days of VOC treatment, many metabolites were significantly less abundant in the exudates, particularly sugars such as fructose, glucose, and raffinose; sugar-related compounds such as erythritol, galactinol, and glycerate; and most amino acids (Figure 7; Supplemental Table 4). Interestingly, consistent with the observed reduction in indolic defense compounds (Figure 6C and 6E), the defensive metabolite pipecolic acid was also less abundant in exudates from VOC-treated plants than in those from controls. In addition, VOC exposure shifted coumarin profiles; exudation of scopoline and skimmin was reduced, and levels of esculetin and fraxetin increased (Figure 7).

In general, the effects of VOCs on root metabolites and exudates showed opposite trends, particularly for amino acids, which, after 2 days, were less abundant in the roots of VOC-treated plants than in controls but accumulated in the exudates; after 5 days, they were reduced in the exudates and increased in the roots relative to untreated plants. In contrast, in the roots, VOC exposure increased the levels of tricarboxylic acid cycle metabolites, particularly citrate and malate, whereas xylose, raffinose, myo-inositol, β-alanine, and pantoic acid levels in roots were lower than in the controls, as in the exudates. Interestingly, ascorbate and dehydroascorbate accumulated to higher levels in VOC-treated roots than in those of controls, indicating an increased need for antioxidants in roots. In shoots, amino acid accumulation was generally lower than in controls, with the exception of histidine, asparagine, and glutamine, as well as fructose and sugar phosphates, especially after 5 days of VOC treatment. In contrast, tocopherols and some amino acid derivatives accumulated to higher levels (Figure 7). Of particular interest was the increased accumulation of S-methylcysteine in the roots and shoots of VOC-treated plants, consistent with its predicted role as an intermediate in DMDS assimilation. Overall, VOCs emitted by the bacterial community caused large alterations in metabolite profiles in both plant tissues and root exudates, and this seems to facilitate bacterial colonization of plants.

DISCUSSION

VOCs emitted by 16-member SynCom are not a sum of VOCs from individual strains

One major advantage of using a synthetic community is the ability to compare the composition and effects of its VOCs with those of the individual strains. The strains included in 16 SC are

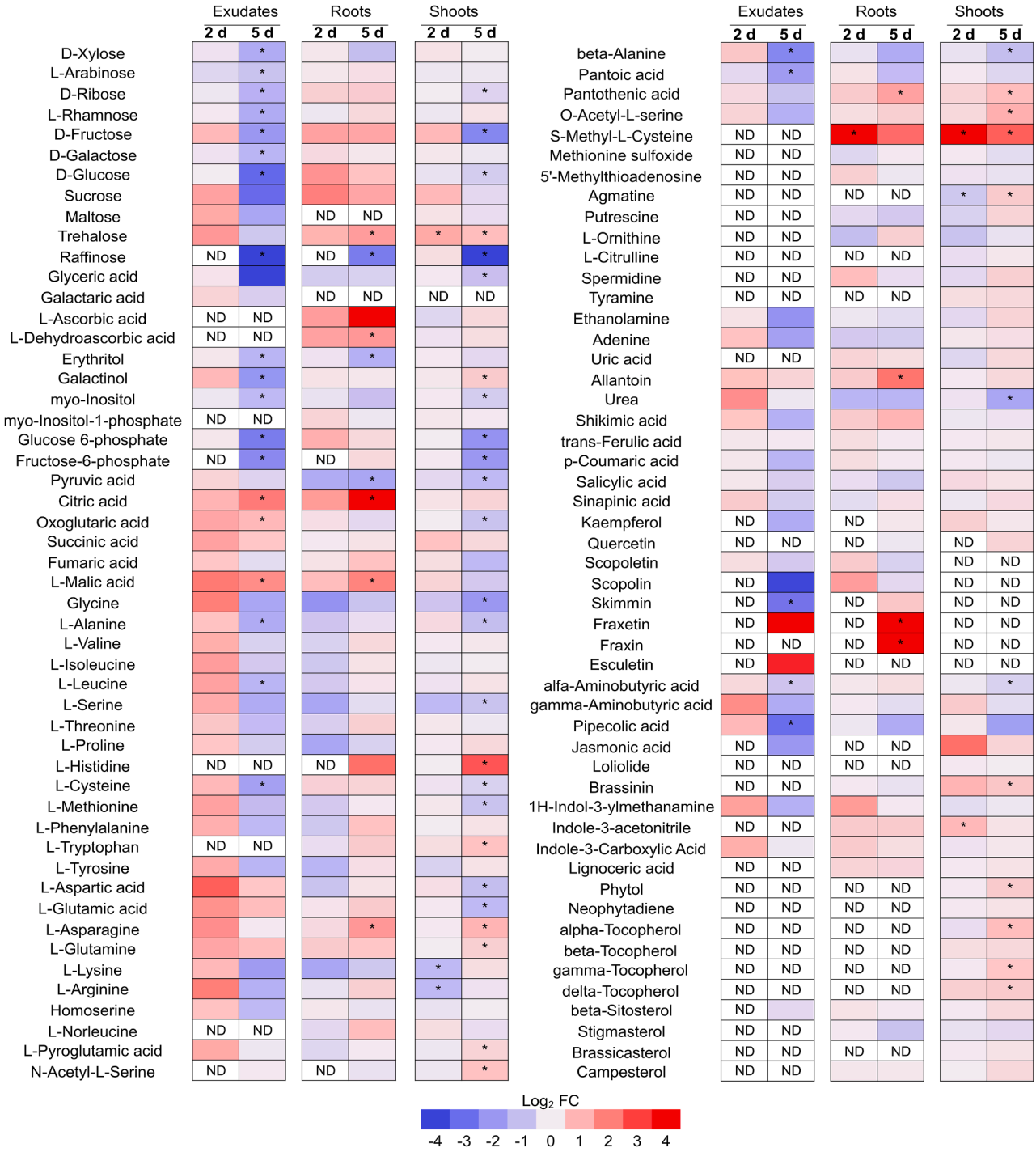

Figure 7. Metabolite analysis of the response of Arabidopsis to 16 SC VOCs.

Arabidopsis plants were grown for 5 days on MS–agar plates and transferred to new plates with or without sharing headspace with 16 SC. After 2 and 5 days, exudates, roots, and shoots were collected and subjected to metabolite analysis by GC–MS of six biological replicates. The heatmaps show the $\log_2$ fold change between VOC-treated and mock-treated plants. Asterisks indicate significant differences between bacterial and mock treatments (Student's *t*-test, $p < 0.05$, $n = 6$). ND, not detected.

taxonomically related to strains with known VOC-mediated effects. For example, the *Pseudomonas* strain R68 and the *Burkholderiales* strains R83 and R29 trigger growth promotion similar to WCS417 and *Burkholderia cepacia*, respectively (Figure 1D) (Vespermann et al., 2007; Zamioudis et al., 2013; Pieterse et al., 2021). Surprisingly, none of the individual strains except R77 affected plant growth and root architecture in the same way as 16 SC. Therefore, it was unclear whether 16 SC emits the sum of the VOCs from individual strains, whether emergent properties arise from interactions among the bacterial strains,

or whether the community's effects are driven by its most abundant strains.

An efficient way to distinguish between these possibilities is through the analysis of drop-out communities (Carlström et al., 2019). We initially selected three strains (R83, R68, and R935) for drop-out analysis because of their high abundance in the community (Figure 2C) and their unique VOC profiles; R68 is the major producer of 1-undecene, and R83 produces diverse terpene compounds (Supplemental Table 1). Notably, although the VOC profiles varied across the drop-out communities, their effects on plants—growth promotion and primary root shortening—remained consistent (Figure 3A and 3B). Omission of individual low-abundance strains, such as R131 or R77, did not alter the PGP effect of the VOCs, which remained stable even in the PGP community, which lacked nine strains compared with 16 SC (Figure 4; Supplemental Figure 4). Thus, despite the changes in community composition and VOC profiles, the effects on the plants remained unchanged. Therefore, the community seems to adapt its VOC production, for example, to compensate for the loss of the three major DMDS producers. This aligns with previous studies in both plant and human microbial communities, where omitting specific strains has consistently affected the abundance of other community members (Carlström et al., 2019; Wang et al., 2023). However, such changes in abundance are not uniformly distributed, e.g., in a human gut microbiome study, removal of individual strains from a 107-member SynCom resulted in a large change in abundance for only 8 strains (Wang et al., 2023). Our results are fully concordant with this pattern, as drop-outs affected only a limited number of other strains. Notably, the abundance of one strain in our SynCom, R77 from the *Caulobacteraceae*, was always increased (Figure 3C). These alterations in 16 SC were compensatory, such that the function of the drop-out communities, as measured by the effect of their VOCs on *Arabidopsis*, remained unchanged compared with the full community.

Similarly, the analysis of a non-PGP community revealed that the community can acquire a new function that is not present in any individual strain (Figure 4). This is possible because the strains forming 16 SC collectively produced 135 different volatiles, but only 55 were present in the VOC profile of the full SynCom. Although this could reflect differences in strain density between pure cultures and the community, it may also represent an emergent property arising from microbe–microbe interactions that affect the metabolism and VOC emissions of the individual strains. An example of a similar emergent function is the ability of several *Streptomyces* strains to grow on chitin as the sole carbon source in a community, but not in pure culture (McClure et al., 2022). Another acquired community function is seen in the maize C7 community, which has been shown to provide plants with much better protection against a fungal pathogen than any individual strain (Niu et al., 2017). Microbe–microbe interactions were also clearly detected in the compositions of the drop-out communities (Figure 3E), likely caused by changes in the bacterial exometabolite balance, a primary determinant of community composition (Getzke et al., 2023). VOCs have also been shown to affect community composition (Yuan et al., 2017). These metabolites, including diffusible antimicrobial compounds, may underlie the dominance of a small number of strains in our community (Figures 4C and 6B). In conclusion, analysis of the non-PGP community suggests that its VOC-mediated phenotypes are emergent and cannot be predicted from the additive effects of the individual strains or even of a few key species.

Sulfur-containing metabolites and growth promotion

Of the 135 compounds detected in the VOC blends, several correlated with the PGP effects (Figure 5A) and promoted growth as pure chemicals (Figure 5B). Interestingly, all tested volatiles with PGP effects—2M5MTF, 2,4-DTP, and DMDS—contain sulfur atoms. Among the 135 VOCs, 24 contain sulfur, and 19 were detected among the 16 SC VOCs, forming 35% of all compounds (Supplemental Table 1). However, many of these compounds were particularly abundant, accounting for 8 of the 10 most abundant 16 SC VOCs. Nevertheless, there was no correlation between the presence of any individual sulfur-containing VOC, or the total number of such VOCs, and the PGP properties of the VOC bouquets, indicating that the final effect on the plant results from an interplay of multiple compounds.

Among the sulfur-containing compounds, DMDS is of particular interest, as it is commonly produced by microbiota and plants and exhibits both PGP and antifungal activities (Meldau et al., 2013; Lin et al., 2021). In our experiments, direct exposure of plants to DMDS also led to growth promotion (Figure 5). DMDS is synthesized via the sulfur metabolism pathway in a wide range of bacteria, presumably through the oxidation of methanethiol, which is derived from methionine by MGL (Weisskopf et al., 2021). Radioisotope tracing has shown that DMDS is incorporated into plant sulfur-containing compounds and proteins; it also promotes growth, especially under low-sulfur conditions (Meldau et al., 2013). DMDS can serve as the sole source of both carbon and sulfur for various bacteria via a pathway involving methanethiol, sulfide, formaldehyde, and formate as intermediates (Figure 5C) (Smith and Kelly, 1988). However, the mechanism of DMDS assimilation in plants is unclear, in contrast to that of hydrogen sulfide, another sulfur-containing volatile, which is directly incorporated into cysteine and can also serve as the sole sulfur source for plant growth (Ausma and De Kok, 2019).

Our analysis of DMDS assimilation strongly suggests that, after its reduction to methanethiol, DMDS is incorporated into O-acetylserine by OAS-TL to form S-methylcysteine. This was supported by the loss of DMDS-induced growth promotion in the *oastlA*, *oastlBC*, and *serat2;2* mutants (Figure 5D), and was confirmed by the metabolite analysis, which showed increased S-methylcysteine accumulation in the roots and shoots of plants exposed to VOCs from DMDS-emitting 16 SC strains (Figure 7). Correspondingly, DMDS induced OAS-TL transcription in tobacco, corroborating the role of OAS-TL in DMDS assimilation (Meldau et al., 2013). The reaction of DMDS with O-acetylserine is well documented in plant sulfur metabolism as part of methionine catabolism (Rébeillé et al., 2006), and S-methylcysteine accumulates to significant levels in some plant species, including common bean, other legumes, onion, and garlic (Chen et al., 1970; Akash et al., 2014; Joshi et al., 2019). Conversion of DMDS to S-methylcysteine increases the availability of reduced sulfur for other metabolic activities and

might, therefore, underlie DMDS-induced growth promotion. The subsequent metabolic path of sulfur contained in S-methylcysteine requires further investigation, but it likely follows the methionine catabolism pathway. Importantly, because some high DMDS emitters, such as R695 and R418, did not promote growth, DMDS cannot be the only growth-promoting component in the VOC blends. Notably, although the *oastlA* and *oastlBC* mutants did not exhibit increased growth after DMDS exposure, they gained fresh weight following incubation with 16 SC (Supplemental Figure 7). This further indicates a complex interplay of multiple compounds in modulating plant responses to bacterial VOCs.

Priming function of bacterial VOCs

Because the drop-out experiments appeared to show that 16 SC adapts its emitted VOCs to induce a consistent effect on plant growth, the VOCs must also serve a function for the bacterial community itself. One explanation is that enhanced plant growth increases the availability of organic carbon for the microorganisms and expands the endophytic space (Weisskopf et al., 2021). However, our experiments revealed additional traits affected by the bacterial VOCs that benefit the microbiota. The reduction in the accumulation of defensive metabolites in the plants and/or root exudates, such as camalexin, glucosinolates, pipecolic acid, salicylic acid, scopolin, and skimmin, may facilitate colonization (Figures 6 and 7). This may seem counterintuitive, because camalexin has been shown to be necessary for plant interactions with beneficial bacteria, i.e., low camalexin was associated with loss of growth promotion (Koprivova et al., 2019). However, the function of camalexin remains unclear, and low camalexin levels might actually lead to greater bacterial proliferation and thus stronger biotic stress, negating the growth benefits. Indeed, the loss of indolic phytoalexins (such as camalexin and indolic glucosinolates) in the *Arabidopsis cyp79B2 cyp79B3* mutant caused otherwise growth-promoting endophytic fungi (*Sebacina vermifera*, *Piriformospora indica*, and *Colletotrichum tofieldiae*) to grow extensively in plant tissues, inhibiting plant growth and even causing plant death (Lahrmann et al., 2015; Hiruma et al., 2016). In addition, because bacterial root colonization triggers an initial defense response that includes the production of reactive oxygen species (Teixeira et al., 2021), the resulting accumulation of ascorbate in roots and tocopherol in shoots might prime the plants and reduce the effects of reactive oxygen species. However, VOCs affect plant metabolism and exudation to a much greater extent than defense compounds alone. The rapid stimulation of the exudation of many primary metabolites, including sugars and amino acids, increases carbon availability for bacteria and may promote colonization (Figure 7). In contrast, the reduced exudation of these metabolites after 5 days may result from increased bacterial growth in the plants or from a regulatory mechanism that limits the attractiveness of the rhizosphere to further microorganisms.

Indeed, bacterial VOCs strongly affected both primary and secondary plant metabolism, and plants exposed to such VOCs ultimately assembled an altered microbial community (Figure 6). This is interesting because, traditionally, only plant-derived VOCs have been implicated as factors in microbiome assembly (Liu and Brettell, 2019). For example, the sand sedge *Carex arenaria* changes its volatile profile following fungal infection, to specifically attract bacteria with antifungal properties (Schulz-Bohm et al., 2018). VOCs can also coordinate microbiome assembly in neighboring plants, as demonstrated in tomato, in which exposure to a β-caryophyllene signal alters root exudate composition, leading to synchronization of the assembled microbiome (Kong et al., 2021). Such signaling also occurs between different plant species; VOCs from potato and onion affect *Pseudomonas* and *Bacillus* recruitment in the tomato rhizosphere, thereby promoting growth (Zhou et al., 2024). Interestingly, the active compound in these cases was dipropyl disulfide, a sulfur-containing volatile with effects similar to those observed for DMDS or 2,4-DTP in our study. Fungi also emit VOCs that modulate bacterial metabolism; for example, VOCs from the fungal pathogen *Fusarium culmorum* induce extensive transcriptional alterations in *Serratia plymuthica*, leading to synthesis of the volatile terpene compound sodorifen (Schmidt et al., 2017). The effects of bacterial VOCs on other bacteria have received less attention. VOCs from *Bacillus amyloliquefaciens* NJN-6 have been shown to alter the composition of soil bacterial and fungal communities (Yuan et al., 2017); however, the effect on plant colonization was not studied. Our findings add a new perspective to the increasing knowledge of how plants shape their microbiome; it seems that microbe assembly might be controlled not only by the plant but also by the microbes themselves. Whether this mechanism can be exploited to predict or engineer plant-associated microbial communities remains to be investigated. To better understand how bacterial communities prime plants for colonization, the mechanisms of action of individual VOCs must be investigated—both alone and in combination—in plants and in the bacterial community, using multi-omics approaches and pathway manipulations. In addition, because our experiments were performed under controlled conditions on agar plates, the applicability of these results to natural soil ecosystems and over longer time scales requires validation.

In summary, our work highlights that VOCs produced by bacterial communities are likely important for plant–microbe communication and for shaping bacterial community composition. We showed that a bacterial community emits a distinct VOC bouquet that differs from the sum of the VOCs produced by its individual members. We demonstrated that changes in community composition modulate VOC chemical profiles but have minimal effects on VOC-mediated PGP. We identified several VOCs from 16 SC that exhibit PGP and proposed a mechanism by which DMDS, one of the major VOCs, exerts its PGP effect. We also showed that the ecological function of these VOCs seems to be the priming of plants for bacterial colonization by altering in root exudates and suppressing defense metabolites. The ability to manipulate plant performance via bacterial VOCs, independent of contact-dependent plant–microbe interactions, represents an exciting and novel opportunity for improving plant health and may lead to a deeper molecular understanding of the mechanisms that drive overall plant performance under field conditions.

MATERIALS AND METHODS

Plant material and growth conditions

A. thaliana WT ecotype Columbia-0 (Col-0) was used for all experiments. For the DMDS experiments, the mutant lines *oastlA* and *oastlBC* (SP1960,

SALK_021183, SALK_000860; Heeg et al., 2008) were obtained from R. Hell, University of Heidelberg, and *serat2;2* (Kazusa_KG752), *sbp1* (SALK_058073), and *mgl* (SALK_103805) were obtained from R. Hoefgen, MPI Golm. Seeds were surface-sterilized for 5 min with 70% ethanol, followed by a brief wash with 100% ethanol. Sterilized seeds were dried and sown on square plates (Greiner, 120 × 120 mm) containing half-strength Murashige and Skoog medium (½ MS) without sucrose and with 0.8% Bacto Agar (pH 5.8). Plates were sealed with Micropore tape and kept in the dark at 4°C for 2–3 days for stratification, then transferred vertically to a growth chamber (16 h light/8 h dark cycle, 21°C/19°C, 100 μmol/m^2/s) for germination for 5 days.

Bacterial growth conditions

The synthetic community of 16 strains (16 SC) was derived from the SynCom At-SC3 (Wippel et al., 2021), with minor changes: Root1221 was replaced by Root29, and Root1485 was replaced by Root418. *P. simiae* WCS417 (Pieterse et al., 2021) was used as a positive control. Bacterial strains were cultured at 28°C on solid medium containing 15 g/l tryptic soy broth (TSB) (Sigma-Aldrich) and 18 g/l Bacto Agar. Information on individual strains can be found at At-RSPHERE (http://www.at-sphere.com/) (Bai et al., 2015). Prior to the experiments, liquid cultures were started from single bacterial colonies in 4 ml liquid TSB and incubated overnight at 28°C with shaking.

For VOC profiling of single strains, overnight cultures were diluted to OD_{600} = 1 in 0.9% sodium chloride and 100 μl of each culture was inoculated onto 1 ml of solid medium containing 15 g/l TSB and 18 g/l Bacto Agar in 10 ml sterile glass headspace vials with crimp caps, then incubated at 22°C. To prepare the SynComs, 50 μl each of the 16 bacterial strains (OD_{600} = 1) were combined and vortexed briefly, then 100 μl of the mixture was used for inoculation. The bacteria were cultured under a photosynthetic photon flux density of 100 μmol m^{-2} s^{-1} during a 16 h photoperiod to match the conditions used for the plate-based system. The duration of cultivation is specified in the individual experiments.

Co-cultivation of plants and bacteria

For the VOC experiments, warm ½ MS medium containing 10 g/l Bacto Agar was poured into square Petri dishes (Greiner, 120 × 120 mm), with a small Petri dish lid (Greiner, 35 × 10 mm) positioned at the center of the bottom part of the plate (Supplemental Figure 1A). The small dish was filled with 4 ml TSB agar medium and allowed to solidify. Five-day-old Col-0 seedlings were placed approximately 1 cm below the top of the square plate. For NBC and combined experiments, 100 μl of bacterial culture (OD_{600} = 1, in 0.9% NaCl; individual strains or 16 SC SynCom) were added to the small Petri dish. For controls and DBC experiments, 0.9% NaCl was added to the small TSB dish. For DBC, we followed a previously established protocol (Ma et al., 2021). In brief, strains were adjusted to OD_{600} = 0.2 using 0.9% NaCl, and 150 μl of each bacterial culture was added to 50 ml of 40°C warm ½ MS agar medium to yield a final density of OD_{600} = 0.0005. The mixture was poured into a square Petri dish and stored at room temperature overnight before seedling transfer. For the control treatment, 150 μl of 0.9% NaCl was added to 50 ml of ½ MS agar medium at 40°C. All plates were sealed with Micropore tape after inoculation and placed vertically in random order in a growth chamber (16 h light/8 h dark cycle, 21°C/19°C, 100 μmol/m^2/s). Pictures were taken after 10 days of VOC exposure (15-day-old seedlings), after which the plants were harvested for fresh weight and metabolite analyses. PRL and LRN were quantified manually from the photographs using ImageJ (Fiji) (Schindelin et al., 2012).

Bacterial profiling

Bacterial DNA for community profiling of pure SynComs was isolated via alkaline lysis. A streak of bacteria was resuspended in 200 μl of 0.9% NaCl, and 12 μl of the suspension was added to 20 μl of buffer I (25 mM NaOH, 0.2 mM EDTA(Na) [pH 12]), mixed by pipetting, and incubated at 94°C for 30 min. To neutralize the pH, 20 μl of buffer II (40 mM Tris–HCl [pH 7.46]) was added. The communities were profiled by amplicon sequencing of the variable V5–V7 regions of the bacterial 16S rRNA gene. Library preparation for Illumina MiSeq sequencing was performed as described previously (Durán et al., 2018). In all experiments, sample multiplexing was performed using double-indexing (barcoded forward and reverse primers for 16S rRNA gene amplification). Amplicon sequencing data were demultiplexed according to their barcode sequences using the QIIME pipeline (Caporaso et al., 2010). Quality-filtered, merged paired-end reads were aligned to reference sequences extracted from the whole-genome assemblies of each strain included in a SynCom, using Rbec (v1.0.0) (Zhang et al., 2021). A count table was generated, RAs were calculated, and these were used for downstream diversity analyses in R (v4.0.3) with the *vegan* package (v2.5–6; *vegdist* function with method = "bray" for Bray–Curtis dissimilarities). Amplicon data were visualized using the *ggplot2* package (v3.3.0) (Wickham, 2016). To quantitatively compare the RAs of individual strains in drop-out SynComs vs. the 16-member SynCom, reads corresponding to the omitted strain were removed from the count table of the full SynCom samples prior to RA calculation.

For priming experiments, DNA was extracted from plant roots using the FastDNA SPIN Kit for Soil (MP Biomedicals, Solon). DNA was eluted with 40 μl of nuclease-free water. The rRNA amplification, library preparation, amplicon sequencing, and raw data generation were performed by Novogene.

VOC profiling of bacterial strains and communities

VOCs were analyzed using a Trace 1300 gas chromatograph coupled with a Q Exactive GC Orbitrap tandem mass spectrometer (Thermo Fisher). One milliliter of the gas phase was directly injected using a TriPlus RSH Autosampler (syringe temperature 100°C; Thermo Fisher) into the injection port (inlet temperature 200°C, splitless time 0.8 min, purge flow rate 5.0 ml/min, split flow rate 10.0 ml/min) connected to a TG-5SilMS GC column (30 m × 0.25 mm × 0.25 μm; Thermo Fisher) with helium as the carrier gas at a constant flow rate of 1 ml/min.

VOCs were collected using an SPME fiber assembly (divinylbenzene/carboxen/polydimethylsiloxane [DVB/CAR/PDMS], film thickness 50/30 μm, length 1 cm; Supelco) coupled with an SPME fiber holder (Supelco). The fiber was exposed to the headspace in the vial for 35 min at 22°C to absorb VOCs, then manually inserted into the injection port for 5 min (inlet temperature 250°C, splitless time 4 min, purge flow rate 5.0 ml/min, split flow rate 10.0 ml/min) connected to a TG-5SilMS GC column with helium as the carrier gas at a constant flow rate of 1 ml/min. The column was heated to 320°C between samples.

Metabolites were separated over a 23-min gradient (held at 30°C for 5 min, then increased at 10°C/min until 260°C, then a 2-min hold) and ionized using electron ionization mode (electron energy 70 eV, emission current 50 μA, transfer line and ion source temperature 250°C). The mass spectrometer operated in full scan mode (resolution 60 000, scan range *m/z* 30–500) with automatic maximum injection time, automatic gain control set to 1e6, and internal lock-mass calibration using the background ion $C_5H_{15}O_3Si_3$ (*m/z* 207.0323).

Data were analyzed using Compound Discoverer 3.3 (Thermo Fisher) and searched against the NIST2014 and GC-Orbitrap Metabolomics libraries (peak detection settings: mass tolerance, 5 ppm; TIC threshold, 10,000; S/N threshold, 3; smoothing, 9; ion overlap window, 90%; group compound settings: RT tolerance, 6 s). Retention indices were calculated using a saturated alkane standard solution (C8–C40). The metabolites were annotated using spectral similarity and retention index comparison. The detectable molecular ion was also considered during the identification. Only metabolites that met the identification criteria (score > 75 and ΔRI < 2%) were retained. Due to the structural diversity of terpenes, only molecular composition was reported. The identification of DMDS and

1-undecene was confirmed by comparison with the corresponding standards. The final evaluation was performed by manual inspection using Skyline 19.1 (Pino et al., 2020). Only peaks fulfilling stringent criteria (absent in blanks and with at least three specific fragment ions) were retained.

Pure compound application

DMDS (Sigma-Aldrich), 2-methyl-5-(methylthio)furan (Thermo Scientific), 2,4-dithiapentane (Sigma-Aldrich), and S-methyl thiobutyrate (Thermo Scientific) were diluted to concentrations of 10–500 μM in ethanol. A cotton bud was placed inside a TSA-containing small Petri dish within the VOC plate system (Supplemental Figure 1A), and 50 μl of each solution was used, with 50 μl of ethanol as the control. 1-Undecene (Sigma-Aldrich) was diluted in chloroform (Sigma-Aldrich), and 50 μl was used in the same manner, with 50 μl of chloroform as the control. The plants were then grown for another 10 days while sealed with microporous tape, as in the bacterial culture experiments.

Priming experiment

Five-day-old plants were transferred to NBC plates (Supplemental Figure 1A) inoculated with 16 SC, as described above, or with sterile medium as a control, and grown for 5 days. Both VOC-treated and untreated plants were then transferred to DBC plates containing 16 SC and cultivated for an additional 7 days. As a control, mock-treated plants were transferred to plates without bacterial inoculation. During harvesting, root material was collected under sterile conditions. Roots were washed with sterile 10 mM $MgSO_4$, transferred to Lysing Matrix E tubes, flash-frozen in liquid nitrogen, and stored at −80°C for bacterial DNA extraction, as described in the community profiling section.

Analysis of defense compounds

Camalexin was extracted from ∼20 mg of shoot tissue (fresh weight) in 100 μl of dimethylsulfoxide for 20 min with shaking at 1,000 rpm. After centrifugation for 20 min at maximum speed, 20 μl was injected into a Thermo Scientific Dionex UltiMate 3000 HPLC system equipped with a Waters Spherisorb ODS-2 column (250 mm × 4.6 mm, 5 μm). Samples were resolved using a gradient of 0.01% (v/v) formic acid (solvent A) and a mixture of 98% (v/v) acetonitrile, 2% (v/v) water, and 0.01% (v/v) formic acid (solvent B). The gradient program was as follows: 97% A for 5 min; 90% A in 5 min; 40% A in 8 min; 20% A in 2 min; 0% A in 20 min and held at 0% A for 10 min; 100% A in 2.5 min and held at 100% A for 3.5 min; 97% A in 2 min and held at 97% A for 2 min. Camalexin was detected using a fluorescence detector with excitation at 318 nm and emission at 368 nm (sensitivity set to 3), as described in Koprivova et al. (2019).

Glucosinolates were determined in shoots using the protocol from Dietzen et al. (2020). In brief, ∼25 mg of tissue was homogenized in 500 μl of hot (70°C) 70% methanol in water, with 2.5 nmol sinigrin used as an internal standard. The extract was incubated at 70°C for 45 min, centrifuged, and loaded onto columns containing 0.5 ml of DEAE-Sephadex A-25. Columns were washed twice with 0.5 ml H_2O and twice with 0.02 M sodium acetate. Then, 75 μl of sulfatase preparation (30 U) was added to each column and incubated overnight. Desulfo-glucosinolates were eluted twice with 0.5 ml of sterile H_2O, followed by a final elution with 0.25 ml. The combined eluates were analyzed by HPLC (Spherisorb ODS-2, 250 × 4.6 mm, 5 μm; Waters) using a gradient of acetonitrile in water and detected by UV absorption at 229 nm. Glucosinolates were quantified using the internal standard and response factors as described in Dietzen et al. (2020).

Exudate analysis

Plants transferred to NBC conditions for priming with 16 SC were used for exudate collection. After 2 or 5 days of VOC exposure, the seedlings were transferred into 12-well plates containing 1 ml of sterile Milli-Q water and incubated for 2 h. The 1 ml exudates were collected and flash-frozen in liquid nitrogen. Roots and shoots were separated and frozen for subsequent metabolic analysis.

Exudate samples were spiked with [^{13}C]L-valine for internal calibration and dried in a speed-vacuum concentrator. Samples were derivatized using 10 μl of methoximation solution (40 mg methoxyamine hydrochloride in 1 ml pyridine) and incubated for 90 min at 30°C with continuous shaking. Then, 40 μl of silylation solution (N-methyl-N-trimethylsilyltrifluoroacetamide) was added, and the mixture was incubated for 30 min at 37°C with continuous shaking, followed by GC–MS analysis.

Metabolite analysis and GC–MS

Root and shoot samples were lyophilized and homogenized in a RETSCH mill using grinding balls (5 min, 30 Hz). Homogenized plant tissue (six biological replicates per condition) was extracted using 0.3 ml of pre-cooled (−20°C) MTBE/methanol (3:1, v/v) spiked with [^{13}C]L-valine, following Berková et al. (2024) with minor modifications. The extracts were vortexed using a RETSCH mill (2 min, 30 Hz, pre-cooled rack), then sonicated for 15 min in an ice-cooled sonication bath. Metabolites were extracted overnight at −20°C, and then the sonication and vortexing steps were repeated. Samples were centrifuged for 10 min at 10 000 *g* at 4°C, and the supernatant was transferred to new 2 ml microcentrifuge tubes. The precipitated pellet was washed with 0.15 ml of methanol and vortexed using a RETSCH mill (2 min, 30 Hz, pre-cooled rack). Samples were centrifuged again for 10 min at 10 000 *g* at 4°C, and the supernatant was combined with the initial supernatant. The combined sample was mixed, aliquoted into new 1.5 ml tubes, and dried in a speed-vacuum concentrator. Samples were dissolved in 15 μl of pyridine and derivatized by incubation with 60 μl of silylation solution (N-methyl-N-trimethylsilyltrifluoroacetamide) for 30 min at 37°C with continuous shaking.

Derivatized metabolites from plant tissue and exudates were injected onto a TG-5SILMS GC column (30 m × 0.25 mm × 0.25 μm; Thermo Fisher), separated using a 28 min temperature gradient (70°C–320°C), and ionized using electron ionization mode (electron energy, 70 eV; emission current, 50 μA; transfer line and ion source temperature, 250°C) (Dufková et al., 2023). Data were analyzed using Compound Discoverer 3.3 (Thermo Fisher; peak detection, 5 ppm; TIC threshold, 25,000; S/N threshold, 3) and searched against the NIST2023 library, the GC-Orbitrap metabolomics library, and an in-house library. Only metabolites that met the identification criteria (score > 75 and ΔRI < 2%) were retained. Quantitative differences were validated using manual peak assignment in Skyline 19.1 (Pino et al., 2020).

Statistical analysis

Pairwise comparisons were performed using two-tailed Student's *t*-tests in Microsoft Excel (treatment mean vs. control mean). GraphPad version 10 was used for Shapiro–Wilk normality tests and to conduct one-way ANOVA with Tukey's HSD (honestly significant difference) *post hoc* pairwise *t*-tests when ANOVA assumptions were met. Alternatively, either the Kruskal–Wallis test or the Welch and Brown–Forsythe tests, followed by Dunnett's test, were performed. Letters and asterisks (*) indicate statistically significant differences between means ($p < 0.05$). Graphs were generated using GraphPad versions 8.02 and 10, R, or Excel. For boxplots, the central bar indicates the median, the lower and upper box limits indicate the 25th and 75th percentiles, respectively, whiskers indicate the minimum and maximum values, and closed dots indicate individual samples. PCA analyses were performed in ClustVis (Metsalu and Vilo, 2015). The data were derived from 4 independent Petri dishes, each containing 10 plants, and all experiments were independently repeated at least twice.

DATA AVAILABILITY

All original data and materials will be provided by the corresponding authors upon request.

FUNDING

T.G.A. is funded by the Max Planck Society (MPG) and the Sofja Kovalevskaja program of the Alexander von Humboldt Foundation. K.W. is funded through the DFG (German Research Foundation) priority program SPP2125 DECRyPT – project 466384294. S.K. and A.K. are funded by the DFG under Germany's Excellence Strategy – EXC 2048/1 – project 390686111 and SPP2125 DECRyPT – project 401836049. G.M.T. thanks the International Max Planck Research School on "Understanding Complex Plant Traits Using Computational and Evolutionary Approaches" and SPP2125 DECRyPT – project 401836049 for support. M.B. and M.Č. acknowledge support from the Czech-German mobility project 8J23DE004. We also thank the German Academic Exchange Service (DAAD) for funding G.M.T.'s stay at Mendel University in Brno – project 57655738.

ACKNOWLEDGMENTS

We thank Bart Boesten (MPI-PZ) for technical assistance with bacterial profiling and Irene Klinkhammer (University of Cologne) for technical assistance with metabolite analyses. We thank Corné Pieterse (Utrecht University) for providing the WCS417 strain, Rüdiger Hell (University of Heidelberg) and Rainer Höfgen (MPI Golm) for seeds of the mutants *oastlA*, *oastlBC*, *mgl*, *sbp1*, and *serat2;2*, respectively. We also thank Ka-Wai Ma (MPI-PZ) for insightful discussions. The authors declare no competing interests.

AUTHOR CONTRIBUTIONS

G.M.T., T.G.A., R.A.C., and S.K. conceptualized the project. G.M.T., T.G.A., and S.K. designed the experiments. G.M.T. conducted the experiments. G.M.T. and M.B. analyzed the data, and T.G.A. and S.K. supervised the project. K.W. and L.R. analyzed the bacterial profiling experiments. M.B. and M.Č. performed GC–MS and analyzed VOC and metabolite profiles. A.K. analyzed defense compounds. G.M.T. drafted the manuscript. G.M.T., K.W., M.B., M.Č., and S.K. generated figures. S.K. edited the manuscript. All authors read and approved the final manuscript.

SUPPLEMENTAL INFORMATION

Supplemental information is available at *Plant Communications Online*.

Received: August 24, 2024
Revised: February 26, 2025
Accepted: May 2, 2025
Published: May 7, 2025

REFERENCES

Abis, L., Loubet, B., Ciuraru, R., Lafouge, F., Houot, S., Nowak, V., Tripied, J., Dequiedt, S., Maron, P.A., and Sadet-Bourgeteau, S. (2020). Reduced microbial diversity induces larger volatile organic compound emissions from soils. Sci. Rep. **10**:6104. https://doi.org/10.1038/s41598-020-63091-8.

Akash, M.S.H., Rehman, K., and Chen, S. (2014). Spice plant Allium cepa: Dietary supplement for treatment of type 2 diabetes mellitus. Nutrition **30**:1128–1137. https://doi.org/10.1016/J.NUT.2014.02.011.

Ausma, T., and De Kok, L.J. (2019). Atmospheric H2S: Impact on plant functioning. Front. Plant Sci. **10**:743. https://doi.org/10.3389/fpls.2019.00743.

Bai, Y., Müller, D.B., Srinivas, G., Garrido-Oter, R., Potthoff, E., Rott, M., Dombrowski, N., Münch, P.C., Spaepen, S., Remus-Emsermann, M., et al. (2015). Functional overlap of the Arabidopsis leaf and root microbiota. Nature **528**:364–369. https://doi.org/10.1038/nature16192.

Basak, A.K., Piasecka, A., Hucklenbroich, J., Türksoy, G.M., Guan, R., Zhang, P., Getzke, F., Garrido-Oter, R., Hacquard, S., Strzałka, K., et al. (2024). ER body-resident myrosinases and tryptophan specialized metabolism modulate root microbiota assembly. New Phytol. **241**:329–342. https://doi.org/10.1111/NPH.19289.

Beck, H.C., Hansen, A.M., and Lauritsen, F.R. (2003). Novel pyrazine metabolites found in polymyxin biosynthesis by Paenibacillus polymyxa. FEMS Microbiol. Lett. **220**:67–73. https://doi.org/10.1016/S0378-1097(03)00054-5.

Berková, V., Berka, M., Štěpánková, L., Kováč, J., Auer, S., Menšíková, S., Ďurkovič, J., Kopřiva, S., Ludwig-Müller, J., Brzobohatý, B., et al. (2024). The fungus Acremonium alternatum enhances salt stress tolerance by regulating host redox homeostasis and phytohormone signaling. Physiol. Plantarum **176**:e14328. https://doi.org/10.1111/ppl.14328.

Blom, D., Fabbri, C., Connor, E.C., Schiestl, F.P., Klauser, D.R., Boller, T., Eberl, L., and Weisskopf, L. (2011). Production of plant growth modulating volatiles is widespread among rhizosphere bacteria and strongly depends on culture conditions. Environ. Microbiol. **13**:3047–3058. https://doi.org/10.1111/j.1462-2920.2011.02582.x.

Bulgarelli, D., Schlaeppi, K., Spaepen, S., Ver Loren van Themaat, E., and Schulze-Lefert, P. (2013). Structure and Functions of the Bacterial Microbiota of Plants. Annu. Rev. Plant Biol. **64**:807–838. https://doi.org/10.1146/annurev-arplant-050312-120106.

Caporaso, J.G., Kuczynski, J., Stombaugh, J., Bittinger, K., Bushman, F.D., Costello, E.K., Fierer, N., Peña, A.G., Goodrich, J.K., Gordon, J.I., et al. (2010). QIIME allows analysis of high-throughput community sequencing data. Nat. Methods **7**:335–336. https://doi.org/10.1038/nmeth.f.303.

Carlström, C.I., Field, C.M., Bortfeld-Miller, M., Müller, B., Sunagawa, S., and Vorholt, J.A. (2019). Synthetic microbiota reveal priority effects and keystone strains in the Arabidopsis phyllosphere. Nature Ecology and Evolution **3**:1445–1454. https://doi.org/10.1038/s41559-019-0994-z.

Castrillo, G., Teixeira, P.J.P.L., Paredes, S.H., Law, T.F., De Lorenzo, L., Feltcher, M.E., Finkel, O.M., Breakfield, N.W., Mieczkowski, P., Jones, C.D., et al. (2017). Root microbiota drive direct integration of phosphate stress and immunity. Nature **543**:513–518. https://doi.org/10.1038/NATURE21417.

Chen, D.M., Nigam, S.N., and McConnell, W.B. (1970). Biosynthesis of Se-methylselenocysteine and S-methylcysteine in Astragalus bisulcatus. Can. J. Biochem. **48**:1278–1283. https://doi.org/10.1139/O70-197.

Chiappero, J., Cappellari, L.d.R., Sosa Alderete, L.G., Palermo, T.B., Banchio, E., and Banchio, E. (2019). Plant growth promoting rhizobacteria improve the antioxidant status in Mentha piperita grown under drought stress leading to an enhancement of plant growth and total phenolic content. Ind. Crop. Prod. **139**:111553. https://doi.org/10.1016/J.INDCROP.2019.111553.

Dietzen, C., Koprivova, A., Whitcomb, S.J., Langen, G., Jobe, T.O., Hoefgen, R., and Kopriva, S. (2020). The Transcription Factor EIL1 Participates in the Regulation of Sulfur-Deficiency Response. Plant Physiol. **184**:2120–2136. https://doi.org/10.1104/pp.20.01192.

Dufková, H., Berka, M., Psota, V., Brzobohatý, B., and Černý, M. (2023). Environmental impacts on barley grain composition and longevity. J. Exp. Bot. **74**:1609–1628. https://doi.org/10.1093/jxb/erac498.

Durán, P., Thiergart, T., Garrido-Oter, R., Agler, M., Kemen, E., Schulze-Lefert, P., and Hacquard, S. (2018). Microbial Interkingdom Interactions in Roots Promote Arabidopsis Survival. Cell **175**:973–983.e14. https://doi.org/10.1016/j.cell.2018.10.020.

Fincheira, P., and Quiroz, A. (2018). Microbial volatiles as plant growth inducers. Microbiol. Res. **208**:63–75. https://doi.org/10.1016/j.micres.2018.01.002.

Getzke, F., Amine Hassani, M., Crüsemann, M., Malisic, M., Zhang, P., Ishigaki, Y., Böhringer, N., Fernández, A.J., Wang, L., Ordon, J., et al. (2023). Cofunctioning of bacterial exometabolites drives root microbiota establishment. Proceedings of the National Academy of Sciences of the United States of America **120**:e2221508120. https://doi.org/10.1073/pnas.2221508120.

Gfeller, A., Fuchsmann, P., De Vrieze, M., Gindro, K., and Weisskopf, L. (2022). Bacterial Volatiles Known to Inhibit Phytophthora infestans Are Emitted on Potato Leaves by Pseudomonas Strains. Microorganisms **10**:1510. https://doi.org/10.3390/microorganisms10081510.

Groenhagen, U., Baumgartner, R., Bailly, A., Gardiner, A., Eberl, L., Schulz, S., and Weisskopf, L. (2013). Production of Bioactive Volatiles by Different Burkholderia ambifaria Strains. J. Chem. Ecol. **39**:892–906. https://doi.org/10.1007/S10886-013-0315-Y/FIGURES/6.

Groenhagen, U., Maczka, M., Dickschat, J.S., and Schulz, S. (2014). Streptopyridines, volatile pyridine alkaloids produced by Streptomyces sp. FORM5. Beilstein J. Org. Chem. **10**:1421–1432. https://doi.org/10.3762/bjoc.10.146.

Harbort, C.J., Hashimoto, M., Inoue, H., Niu, Y., Guan, R., Rombolà, A. D., Kopriva, S., Voges, M.J.E.E.E., Sattely, E.S., Garrido-Oter, R., et al. (2020). Root-Secreted Coumarins and the Microbiota Interact to Improve Iron Nutrition in Arabidopsis. Cell Host Microbe **28**:825–837.e6. https://doi.org/10.1016/J.CHOM.2020.09.006.

Heeg, C., Kruse, C., Jost, R., Gutensohn, M., Ruppert, T., Wirtz, M., and Hell, R. (2008). Analysis of the Arabidopsis O-Acetylserine(thiol) lyase Gene Family Demonstrates Compartment-Specific Differences in the Regulation of Cysteine Synthesis. Plant Cell **20**:168–185. https://doi.org/10.1105/TPC.107.056747.

Hiruma, K., Gerlach, N., Sacristán, S., Nakano, R.T., Hacquard, S., Kracher, B., Neumann, U., Ramírez, D., Bucher, M., O'Connell, R. J., et al. (2016). Root Endophyte Colletotrichum tofieldiae Confers Plant Fitness Benefits that Are Phosphate Status Dependent. Cell **165**:464–474. https://doi.org/10.1016/J.CELL.2016.02.028.

Hunziker, L., Bönisch, D., Groenhagen, U., Bailly, A., Schulz, S., and Weisskopf, L. (2015). Pseudomonas Strains Naturally Associated with Potato Plants Produce Volatiles with High Potential for Inhibition of Phytophthora infestans. Appl. Environ. Microbiol. **81**:821–830. https://doi.org/10.1128/AEM.02999-14.

Joshi, J., Saboori-Robat, E., Solouki, M., Mohsenpour, M., and Marsolais, F. (2019). Distribution and possible biosynthetic pathway of non-protein sulfur amino acids in legumes. J. Exp. Bot. **70**:4115–4121. https://doi.org/10.1093/JXB/ERZ291.

Kong, H.G., Song, G.C., Sim, H.J., and Ryu, C.M. (2021). Achieving similar root microbiota composition in neighbouring plants through airborne signalling. ISME J. **15**:397–408. https://doi.org/10.1038/S41396-020-00759-Z.

Koprivova, A., and Kopriva, S. (2022). Plant secondary metabolites altering root microbiome composition and function. Curr. Opin. Plant Biol. **67**:102227. https://doi.org/10.1016/j.pbi.2022.102227.

Koprivova, A., Schuck, S., Jacoby, R.P., Klinkhammer, I., Welter, B., Leson, L., Martyn, A., Nauen, J., Grabenhorst, N., Mandelkow, J. F., et al. (2019). Root-specific camalexin biosynthesis controls the plant growth-promoting effects of multiple bacterial strains. Proc. Natl. Acad. Sci. USA **116**:15735–15744. https://doi.org/10.1073/pnas.1818604116.

Knoester, M., Pieterse, C.M., Bol, J.F., and Van Loon, L.C. (1999). Systemic resistance in Arabidopsis induced by rhizobacteria requires ethylene-dependent signaling at the site of application. Mol. Plant Microbe Interact **12**:720–727. https://doi.org/10.1094/MPMI.1999.12.8.720.

Lahrmann, U., Strehmel, N., Langen, G., Frerigmann, H., Leson, L., Ding, Y., Scheel, D., Herklotz, S., Hilbert, M., and Zuccaro, A. (2015). Mutualistic root endophytism is not associated with the reduction of saprotrophic traits and requires a noncompromised plant innate immunity. New Phytol. **207**:841–857. https://doi.org/10.1111/NPH.13411.

Lamers, J.G., Schippers, B., and Geels, F.P. (1988). Soil-borne diseases of wheat in the Netherlands and results of seed bacterization with pseudomonads against Gaeumannomyces graminis var. tritici, associated with disease resistance. In Cereal Breeding Related to Integrated Cereal Production, M.L. Jorna and L.A.J. Slootmaker, eds. (Wageningen: Pudoc), pp. 134–139.

Lin, Y.T., Lee, C.C., Leu, W.M., Wu, J.J., Huang, Y.C., and Meng, M. (2021). Fungicidal Activity of Volatile Organic Compounds Emitted by Burkholderia gladioli Strain BBB-01. Molecules **26**:745. https://doi.org/10.3390/MOLECULES26030745.

Liu, H., and Brettell, L.E. (2019). Plant Defense by VOC-Induced Microbial Priming. Trends Plant Sci. **24**:187–189. https://doi.org/10.1016/J.TPLANTS.2019.01.008.

Lo Cantore, P., Giorgio, A., and Iacobellis, N.S. (2015). Bioactivity of volatile organic compounds produced by Pseudomonas tolaasii. Front. Microbiol. **6**:156562. https://doi.org/10.3389/FMICB.2015.01082/BIBTEX.

Loo, E.P.I., Tajima, Y., Yamada, K., Kido, S., Hirase, T., Ariga, H., Fujiwara, T., Tanaka, K., Taji, T., Somssich, I.E., et al. (2022). Recognition of Microbe- and Damage-Associated Molecular Patterns by Leucine-Rich Repeat Pattern Recognition Receptor Kinases Confers Salt Tolerance in Plants. Mol. Plant Microbe Interact. **35**:554–566. https://doi.org/10.1094/MPMI-07-21-0185-FI/ASSET/IMAGES/LARGE/MPMI-07-21-0185-FIF7.JPEG.

Ma, K.W., Niu, Y., Jia, Y., Ordon, J., Copeland, C., Emonet, A., Geldner, N., Guan, R., Stolze, S.C., Nakagami, H., et al. (2021). Coordination of microbe–host homeostasis by crosstalk with plant innate immunity. Nat. Plants **7**:814–825. https://doi.org/10.1038/s41477-021-00920-2.

Martins, S.J., Pasche, J., Silva, H.A.O., Selten, G., Savastano, N., Abreu, L.M., Bais, H.P., Garrett, K.A., Kraisitudomsook, N., Pieterse, C.M.J., et al. (2023). The Use of Synthetic Microbial Communities to Improve Plant Health. Phytopathology **113**:1369–1379. https://doi.org/10.1094/PHYTO-01-23-0016-IA/ASSET/IMAGES/LARGE/PHYTO-01-23-0016-IAF3.JPEG.

Martín-Sánchez, L., Singh, K.S., Avalos, M., Van Wezel, G.P., Dickschat, J.S., and Garbeva, P. (2019). Phylogenomic analyses and distribution of terpene synthases among Streptomyces. Beilstein J. Org. Chem. **15**:1181–1193. https://doi.org/10.3762/BJOC.15.115.

McClure, R., Farris, Y., Danczak, R., Nelson, W., Song, H.-S., Kessell, A., Lee, J.-Y., Couvillion, S., Henry, C., Jansson, J.K., et al. (2022). Interaction Networks Are Driven by Community-Responsive Phenotypes in a Chitin-Degrading Consortium of Soil Microbes. mSystems **7**:e0037222. https://doi.org/10.1128/MSYSTEMS.00372-22.

Meldau, D.G., Meldau, S., Hoang, L.H., Underberg, S., Wünsche, H., and Baldwin, I.T. (2013). Dimethyl disulfide produced by the naturally associated bacterium bacillus sp B55 promotes Nicotiana attenuata growth by enhancing sulfur nutrition. Plant Cell **25**:2731–2747. https://doi.org/10.1105/TPC.113.114744.

Metsalu, T., and Vilo, J. (2015). ClustVis: A web tool for visualizing clustering of multivariate data using Principal Component Analysis and heatmap. Nucleic Acids Res. **43**:W566–W570. https://doi.org/10.1093/nar/gkv468.

Niu, B., Paulson, J.N., Zheng, X., and Kolter, R. (2017). Simplified and representative bacterial community of maize roots. Proc. Natl. Acad. Sci. USA **114**:E2450–E2459. https://doi.org/10.1073/PNAS.1616148114.

Peñuelas, J., Asensio, D., Tholl, D., Wenke, K., Rosenkranz, M., Piechulla, B., and Schnitzler, J.P. (2014). Biogenic volatile

emissions from the soil. Plant Cell Environ. **37**:1866–1891. https://doi.org/10.1111/PCE.12340.

Philipp, T.M., Scheller, A.S., Krafczyk, N., Klotz, L.O., and Steinbrenner, H. (2023). Methanethiol: A Scent Mark of Dysregulated Sulfur Metabolism in Cancer. Antioxidants **12**:1780. https://doi.org/10.3390/ANTIOX12091780.

Piechulla, B., Lemfack, M.C., and Kai, M. (2017). Effects of discrete bioactive microbial volatiles on plants and fungi. Plant Cell Environ. **40**:2042–2067. https://doi.org/10.1111/PCE.13011.

Pieterse, C.M.J., Berendsen, R.L., de Jonge, R., Stringlis, I.A., Van Dijken, A.J.H., Van Pelt, J.A., Van Wees, S.C.M., Yu, K., Zamioudis, C., and Bakker, P.A.H.M. (2021). Pseudomonas simiae WCS417: star track of a model beneficial rhizobacterium. Plant Soil **461**:245–263. https://doi.org/10.1007/s11104-020-04786-9.

Pieterse, C.M.J., van Wees, S.C.M., Hoffland, E., van Pelt, J.A., and van Loon, L.C. (1996). Systemic Resistance in Arabidopsis Induced by Biocontrol Bacteria Is Independent of Salicylic Acid Accumulation and Pathogenesis-Related Gene Expression. Plant Cell **8**:1225. https://doi.org/10.2307/3870297.

Pino, L.K., Searle, B.C., Bollinger, J.G., Nunn, B., MacLean, B., and MacCoss, M.J. (2020). The Skyline ecosystem: Informatics for quantitative mass spectrometry proteomics. Mass Spectrom. Rev. **39**:229–244. https://doi.org/10.1002/mas.21540.

Popova, A.A., Koksharova, O.A., Lipasova, V.A., Zaitseva, J.V., Katkova-Zhukotskaya, O.A., Eremina, S.I., Mironov, A.S., Chernin, L.S., and Khmel, I.A. (2014). Inhibitory and Toxic Effects of Volatiles Emitted by Strains of Pseudomonas and Serratia on Growth and Survival of Selected Microorganisms, Caenorhabditis elegans, and Drosophila melanogaster. BioMed Res. Int. **2014**:125704. https://doi.org/10.1155/2014/125704.

Raza, W., Wang, J., Jousset, A., Friman, V.P., Mei, X., Wang, S., Wei, Z., and Shen, Q. (2020). Bacterial community richness shifts the balance between volatile organic compound-mediated microbe–pathogen and microbe–plant interactions. Proc. Biol. Sci. **287**:20200403. https://doi.org/10.1098/rspb.2020.0403.

Raza, W., Wei, Z., Jousset, A., Shen, Q., and Friman, V.-P. (2021). Extended Plant Metarhizobiome: Understanding Volatile Organic Compound Signaling in Plant-Microbe Metapopulation Networks. mSystems **6**:e0084921. https://doi.org/10.1128/MSYSTEMS.00849-21/SUPPL_FILE/REVIEWER-COMMENTS.PDF.

Rébeillé, F., Jabrin, S., Bligny, R., Loizeau, K., Gambonnet, B., Van Wilder, V., Douce, R., and Ravanel, S. (2006). Methionine catabolism in Arabidopsis cells is initiated by a γ-cleavage process and leads to S-methylcysteine and isoleucine syntheses. Proceedings of the National Academy of Sciences of the United States of America **103**:15687–15692. https://doi.org/10.1073/PNAS.0606195103/ASSET/B5D48558-78FA-45F6-A53C-5F369634CD62/ASSETS/GRAPHIC/ZPQ0410637480006.JPEG.

Ryu, C.M., Farag, M.A., Hu, C.H., Reddy, M.S., Wei, H.X., Paré, P.W., and Kloepper, J.W. (2003). Bacterial volatiles promote growth in Arabidopsis. Proc. Natl. Acad. Sci. USA **100**:4927–4932. https://doi.org/10.1073/pnas.0730845100.

Ryu, C.-M., Weisskopf, L., and Piechulla, B. (2020). Bacterial Volatile Compounds as Mediators of Airborne Interactions (Singapore: Springer Singapore). https://doi.org/10.1007/978-981-15-7293-7.

Schindelin, J., Arganda-Carreras, I., Frise, E., Kaynig, V., Longair, M., Pietzsch, T., Preibisch, S., Rueden, C., Saalfeld, S., Schmid, B., et al. (2012). Fiji: an open-source platform for biological-image analysis. Nat. Methods **9**:676–682. https://doi.org/10.1038/nmeth.2019.

Schmidt, R., De Jager, V., Zühlke, D., Wolff, C., Bernhardt, J., Cankar, K., Beekwilder, J., Van Ijcken, W., Sleutels, F., De Boer, W., et al. (2017). Fungal volatile compounds induce production of the secondary metabolite Sodorifen in Serratia plymuthica PRI-2C. Sci. Rep. **7**:862. https://doi.org/10.1038/s41598-017-00893-3.

Schulz, S., and Dickschat, J.S. (2007). Bacterial volatiles: the smell of small organisms. Nat. Prod. Rep. **24**:814–842. https://doi.org/10.1039/B507392H.

Schulz-Bohm, K., Gerards, S., Hundscheid, M., Melenhorst, J., De Boer, W., and Garbeva, P. (2018). Calling from distance: attraction of soil bacteria by plant root volatiles. ISME J. **12**:1252–1262. https://doi.org/10.1038/s41396-017-0035-3.

Smith, N.A., and Kelly, D.P. (1988). Isolation and Physiological Characterization of Autotrophic Sulphur Bacteria Oxidizing Dimethyl Disulphide as Sole Source of Energy. Microbiology **134**:1407–1417. https://doi.org/10.1099/00221287-134-6-1407.

Stringlis, I.A., Yu, K., Feussner, K., De Jonge, R., Van Bentum, S., Van Verk, M.C., Berendsen, R.L., Bakker, P.A.H.M., Feussner, I., and Pieterse, C.M.J. (2018). MYB72-dependent coumarin exudation shapes root microbiome assembly to promote plant health. Proc. Natl. Acad. Sci. USA **115**:E5213–E5222. https://doi.org/10.1073/PNAS.1722335115/SUPPL_FILE/PNAS.1722335115.SD06.XLSX.

Teixeira, P.J.P.L., Colaianni, N.R., Law, T.F., Conway, J.M., Gilbert, S., Li, H., Salas-González, I., Panda, D., Risco, N.M.D., Finkel, O.M., et al. (2021). Specific modulation of the root immune system by a community of commensal bacteria. Plant Biol. **118**:2100678118. https://doi.org/10.1073/pnas.2100678118/-/DCSupplemental.

Trapet, P., Avoscan, L., Klinguer, A., Pateyron, S., Citerne, S., Chervin, C., Mazurier, S., Lemanceau, P., Wendehenne, D., and Besson-Bard, A. (2016). The Pseudomonas fluorescens Siderophore Pyoverdine Weakens Arabidopsis thaliana Defense in Favor of Growth in Iron-Deficient Conditions. Plant Physiol. **171**:675–693. https://doi.org/10.1104/pp.15.01537.

Tyagi, S., Kim, K., Cho, M., Kui, and Lee, J. (2019). Volatile dimethyl disulfide affects root system architecture of Arabidopsis via modulation of canonical auxin signaling pathways. Environ. Sustain. (Singap). **2**:211–216. https://doi.org/10.1007/S42398-019-00060-6.

Vespermann, A., Kai, M., and Piechulla, B. (2007). Rhizobacterial volatiles affect the growth of fungi and Arabidopsis thaliana. Appl. Environ. Microbiol. **73**:5639–5641. https://doi.org/10.1128/AEM.01078-07.

Vorholt, J.A., Vogel, C., Carlström, C.I., and Müller, D.B. (2017). Establishing Causality: Opportunities of Synthetic Communities for Plant Microbiome Research. Cell Host Microbe **22**:142–155. https://doi.org/10.1016/J.CHOM.2017.07.004.

Wang, J., Mei, X., Wei, Z., Raza, W., and Shen, Q. (2021). Effect of bacterial intra-species community interactions on the production and activity of volatile organic compounds. Soil Ecol. Lett. **3**:32–41. https://doi.org/10.1007/s42832-020-0054-2.

Wang, M., Osborn, L.J., Jain, S., Meng, X., Weakley, A., Yan, J., Massey, W.J., Varadharajan, V., Horak, A., Banerjee, R., et al. (2023). Strain dropouts reveal interactions that govern the metabolic output of the gut microbiome. Cell **186**:2839–2852.e21. https://doi.org/10.1016/J.CELL.2023.05.037.

Watanabe, M., Kusano, M., Oikawa, A., Fukushima, A., Noji, M., and Saito, K. (2008). Physiological Roles of the β-Substituted Alanine Synthase Gene Family in Arabidopsis. Plant Physiol. **146**:310–320. https://doi.org/10.1104/PP.107.106831.

Weise, T., Thürmer, A., Brady, S., Kai, M., Daniel, R., Gottschalk, G., and Piechulla, B. (2014). VOC emission of various Serratia species and isolates and genome analysis of Serratia plymuthica 4Rx13. FEMS Microbiol. Lett. **352**:45–53. https://doi.org/10.1111/1574-6968.12359.

Weisskopf, L., Schulz, S., and Garbeva, P. (2021). Microbial volatile organic compounds in intra-kingdom and inter-kingdom interactions.

Nat. Rev. Microbiol. **19**:391–404. https://doi.org/10.1038/s41579-020-00508-1.

Wickham, H. (2016). ggplot2: Elegant Graphics for Data Analysis (New York: Springer-Verlag).

Wippel, K., Tao, K., Niu, Y., Zgadzaj, R., Kiel, N., Guan, R., Dahms, E., Zhang, P., Jensen, D.B., Logemann, E., et al. (2021). Host preference and invasiveness of commensal bacteria in the Lotus and Arabidopsis root microbiota. Nat. Microbiol. **6**:1150–1162. https://doi.org/10.1038/s41564-021-00941-9.

Wirtz, M., and Hell, R. (2006). Functional analysis of the cysteine synthase protein complex from plants: Structural, biochemical and regulatory properties. J. Plant Physiol. **163**:273–286. https://doi.org/10.1016/J.JPLPH.2005.11.013.

Yuan, J., Zhao, M., Li, R., Huang, Q., Raza, W., Rensing, C., and Shen, Q. (2017). Microbial volatile compounds alter the soil microbial community. Environ. Sci. Pollut. Res. Int. **24**:22485–22493. https://doi.org/10.1007/s11356-017-9839-y.

Zamioudis, C., Korteland, J., Van Pelt, J.A., van Hamersveld, M., Dombrowski, N., Bai, Y., Hanson, J., Van Verk, M.C., Ling, H.Q., Schulze-Lefert, P., et al. (2015). Rhizobacterial volatiles and photosynthesis-related signals coordinate MYB72 expression in Arabidopsis roots during onset of induced systemic resistance and iron-deficiency responses. Plant J. **84**:309–322. https://doi.org/10.1111/tpj.12995.

Zamioudis, C., Mastranesti, P., Dhonukshe, P., Blilou, I., and Pieterse, C.M.J. (2013). Unraveling Root Developmental Programs Initiated by Beneficial Pseudomonas spp. Bacteria. Plant Physiol. **162**:304–318. https://doi.org/10.1104/PP.112.212597.

Zhang, H., Zhu, Y., Wang, Y., Jiang, L., Shi, X., and Cheng, G. (2024). Microbial interactions shaping host attractiveness: insights into dynamic behavioral relationships. Curr. Opin. Insect Sci. **66**:101275. https://doi.org/10.1016/j.cois.2024.101275.

Zhang, J., Liu, Y.X., Zhang, N., Hu, B., Jin, T., Xu, H., Qin, Y., Yan, P., Zhang, X., Guo, X., et al. (2019). NRT1.1B is associated with root microbiota composition and nitrogen use in field-grown rice. Nat. Biotechnol. **37**:676–684. https://doi.org/10.1038/S41587-019-0104-4.

Zhang, P., Spaepen, S., Bai, Y., Hacquard, S., and Garrido-Oter, R. (2021). Rbec: a tool for analysis of amplicon sequencing data from synthetic microbial communities. ISME Commun. **1**:73. https://doi.org/10.1038/s43705-021-00077-1.

Zhou, X., Zhang, J., Shi, J., Khashi U Rahman, M., Liu, H., Wei, Z., Wu, F., and Dini-Andreote, F. (2024). Volatile-mediated interspecific plant interaction promotes root colonization by beneficial bacteria via induced shifts in root exudation. Microbiome **12**:207. https://doi.org/10.1186/s40168-024-01914-w.